

Article

# Differential Ozone Responses Identified among Key Rust-Susceptible Wheat Genotypes

Alsayed M. Mashaheet <sup>1,2,\*</sup> , Kent O. Burkey <sup>3</sup> , Costas J. Saitanis <sup>4</sup>,  
Abdelrazek S. Abdelrhim <sup>5</sup> , Rafiullah <sup>6</sup> and David S. Marshall <sup>3</sup> 

<sup>1</sup> Department of Entomology and Plant Pathology, North Carolina State University, Raleigh, NC 27695, USA

<sup>2</sup> Department of Plant Pathology, Faculty of Agriculture, Damanhour University, Damanhour 22511, Egypt

<sup>3</sup> USDA-ARS, Plant Science Research Unit, Raleigh, NC 27695, USA; Kent.Burkey@ars.usda.gov (K.O.B.); david.marshall@ars.usda.gov (D.S.M.)

<sup>4</sup> Lab of Ecology and Environmental Science, Agricultural University of Athens, 11855 Athens, Greece; saitanis@aua.gr

<sup>5</sup> Department of Plant Pathology, Faculty of Agriculture, Minia University, El-Minia 61519, Egypt; Abdelrazek.sharawy@mu.edu.eg

<sup>6</sup> Department of Agriculture, University of Swabi, Khyber Pakhtunkhwa 23561, Pakistan; rafiullah@uoswabi.edu.pk

\* Correspondence: a.mashaheet@dmu.edu.eg; Tel.: +20-122-750-7027

Received: 30 September 2020; Accepted: 23 November 2020; Published: 25 November 2020



**Abstract:** Increasing ambient ozone (O<sub>3</sub>) concentrations and resurgent rust diseases are two concomitant limiting factors to wheat production worldwide. Breeding resilient wheat cultivars bearing rust resistance and O<sub>3</sub> tolerance while maintaining high yield is critical for global food security. This study aims at identifying ozone tolerance among key rust-susceptible wheat genotypes [Rust near-universal susceptible genotypes (RnUS)], as a first step towards achieving this goal. Tested RnUS included seven bread wheat genotypes (Chinese Spring, Line E, Little Club, LMPG 6, McNair 701, Morocco and Thatcher), and one durum wheat line (Rusty). Plants were treated with five O<sub>3</sub> concentrations (CF, 50, 70, 90, and 110 ppb), in two O<sub>3</sub> exposure systems [continuous stirred tank reactors (CSTR) and outdoor-plant environment chambers (OPEC)], at 21–23 Zadoks decimal growth stage. Visible injury and biomass accumulation rate were used to assess O<sub>3</sub> responses. Visible injury data showed consistent order of genotype sensitivity (Thatcher, LMPG 6 > McNair 701, Rusty > Line E, Morocco, Little Club > Chinese Spring). Additionally, leaves at different orders showed differential O<sub>3</sub> responses. Biomass accumulation under O<sub>3</sub> stress showed similar results for the bread wheat genotypes. However, the durum wheat line “Rusty” had the most O<sub>3</sub>-sensitive biomass production, providing a contrasting O<sub>3</sub> response to the tolerance reported in durum wheat. Chinese Spring was the most tolerant genotype based on both parameters and could be used as a source for O<sub>3</sub> tolerance, while sensitive genotypes could be used as sensitive parents in mapping O<sub>3</sub> tolerance in bread wheat. The suitability of visible symptoms and biomass responses in high-throughput screening of wheat for O<sub>3</sub> tolerance was discussed. The results presented in this research could assist in developing future approaches to accelerate breeding wheat for O<sub>3</sub> tolerance using existing breeding materials.

**Keywords:** global food security; resilient wheat; relative growth rate; ozone injury

## 1. Introduction

Increasing ambient ozone (O<sub>3</sub>) concentrations and resurgent rust diseases are two concomitant limiting factors to wheat production worldwide [1,2]. Breeding resilient wheat cultivars bearing O<sub>3</sub> tolerance and rust resistance while maintaining high yield is critical for global food security.

Rust near-universal susceptible genotypes (RnUS) are a common set of test materials used by breeders to assist in the characterization of new rust resistance genes and their introduction into breeding programs during the development of new rust resistant varieties [3–6]. Because of their widespread use in breeding programs, the identification of differential O<sub>3</sub> responses among RnUS wheat genotypes is an important step towards achieving this goal.

O<sub>3</sub> is the most phytotoxic air pollutant that causes a continuum of symptomatic and sub-symptomatic responses [7]. This greenhouse gas is formed in ambient air by photochemical reactions between nitrogen oxides (NO<sub>x</sub>) and non-methane volatile organic compounds [8]. It exerts a high oxidizing power on plants cellular components, such as cuticle, cell walls, and cell membranes [9]. After diffusing into plant leaves, through stomata, O<sub>3</sub> dissolves in the apoplastic fluid [10], generating primary and secondary bursts of reactive oxygen species (ROS) [11,12]. O<sub>3</sub>-induced ROS alter apoplastic and symplastic interfaces, causing structural, biochemical, and physiological changes, known as sub-symptomatic O<sub>3</sub> responses. Under prolonged and/or high O<sub>3</sub> levels, sub-symptomatic O<sub>3</sub> responses lead to the development of O<sub>3</sub> visible symptoms, reduced biomass, and seed yields [13].

Wheat is among the most O<sub>3</sub>-sensitive crops, at all growth stages [14]. O<sub>3</sub> effects on wheat plants include alteration in antioxidant capacity [15], altered stomatal conductance and gas exchange [16–18], increased membrane damage and electrolyte leakage [19], reduced photosynthesis [20–22]. O<sub>3</sub> also causes chlorophyll degradation, chlorotic and/or necrotic visible symptoms, and hastens leaf senescence [23–26]. All these effects of O<sub>3</sub> lead to an overall reduction of wheat biomass, grain yield, and protein content [14,17,18,25,27–30]. Currently, more than 85 million tons of wheat are estimated to be lost due to O<sub>3</sub> stress [31–33].

Although O<sub>3</sub> tolerance of wheat species and varieties has been investigated [31,32,34–37], breeding studies for O<sub>3</sub> tolerance have not been reported. This is due to the lack of reliable screening and the lack of information about the heritability of the O<sub>3</sub> tolerance trait and its potential contribution to genetic gain [38]. Traditional field screening under natural O<sub>3</sub> stress, as part of selection for other traits, is not a suitable selection procedure for breeding O<sub>3</sub>-tolerant wheat varieties [39,40]. Elevated ambient O<sub>3</sub> is a diverse problem, both spatially and temporally. These variations in O<sub>3</sub> levels do not provide the consistent O<sub>3</sub> stress necessary to make progress [40]. The continuous stirred tank reactors (CSTRs) [41,42] and outdoor-plant environment chambers (OPECs) [43] are two systems for providing consistent differential levels of O<sub>3</sub> stress. The identification of molecular markers associated with O<sub>3</sub> tolerance in wheat is a key step for breeding programs [44,45]. These markers could boost breeding efforts via high throughput phenotyping and marker-assisted selection.

The global spread of rust diseases in areas where ambient O<sub>3</sub> occurs at significantly high levels suggests possible interactions between the two factors, and the potential and need for breeding wheat for rust resistance and O<sub>3</sub> tolerance simultaneously. Wheat rusts are serious foliar diseases of wheat, caused by pathogenic fungi (stem rust (Sr) caused by *Puccinia graminis* f. sp. *tritici*; leaf rust (Lr) caused by *Puccinia triticina* Eriks.; stripe rust (Yr) caused by *Puccinia striiformis* f. sp. *tritici*) [46]. These are biotrophic pathogens that require living host tissue for growth, resulting in significant yield reductions [1]. Rust pathogens are one of the most rapidly evolving pathogen groups. They have large population sizes, long-distance air-borne spore dispersal, and both sexual and asexual reproduction [47]. These characteristics enable rust pathogens to have continental and global spread of complex and rapidly evolving populations, usually consisting of multiple races, and consequently overcome resistance genes in the host [48]. This has resulted in global breeding programs for rust resistance, which could serve as a surrogate for breeding for O<sub>3</sub> tolerance when differential O<sub>3</sub> responses are identified among key wheat breeding material. Additionally, the interactions of rust populations and O<sub>3</sub>-stressed wheat plants are not fully understood and require the identification of suitable host material with identified O<sub>3</sub> responses.

The rust near-universally susceptible wheat genotypes (RnUS), commonly referred to as “Rust universal susceptible panel”, allow for unimpeded infection with nearly all rust races [6]. Thus, RnUS are used globally to detect rust infection in nature, and to maintain and increase rust spores under controlled

conditions, without selecting against races. Additionally, RnUS are commonly used to develop biparental mapping populations segregating for rust resistance [5,6,49]. By phenotyping rust resistance and genotyping of these biparental mapping populations, wheat breeders identify and characterize rust resistance genes and the associated molecular markers to be used in marker-assisted selection. The same plant materials and procedures could be used simultaneously for O<sub>3</sub> tolerance, on a global scale; however, no information is available on the RnUS response to O<sub>3</sub> stress.

The objectives of this study were to assess the O<sub>3</sub> responses of eight RnUS based on canopy visible injury responses, as well as growth rates, and the relationship between the two types of responses and their suitability for rapid and reliable screening for O<sub>3</sub> tolerance.

## 2. Materials and Methods

### 2.1. Exposure Systems

Two O<sub>3</sub> exposure experiments were conducted in this study, using two controlled O<sub>3</sub> exposure systems that are considered suitable for delivering the consistent, relevant, and differential O<sub>3</sub> treatments needed to identify O<sub>3</sub> responses of wheat entries. In each of the systems, O<sub>3</sub> was generated by a TG-20 Ozone Generator (Ozone Solutions, Hull, IA, USA), and the O<sub>3</sub> concentrations were monitored by a Model 49C Ozone Analyzer (Thermo Environmental Instruments, Franklin, MA, USA).

#### 2.1.1. Continuous Stirred Tank Reactors (CSTRs)

The first experiment was conducted in cylindrical exposure chambers, known as continuous stirred tank reactors (CSTRs) covered with Teflon film, operating inside a greenhouse provided with activated charcoal-filtered air (CF). Chambers had a single-pass air ventilation system, designed for rapid mixing of gases [41,42]. CF air mixed with steady levels of O<sub>3</sub> entered from the top of the chamber and was continuously stirred with a fan positioned the chamber ceiling. A negative pressure blower system removed the air from the bottom of the chamber, after passing through the plant canopy. Relative humidity was monitored and controlled by adding water vapor under pressure to the air as it entered the chamber. Temperatures were monitored and controlled in the entire greenhouse. A supplemental light source was located over the chamber to compensate for the greenhouse and chamber shading effects.

#### 2.1.2. Outdoor-Plant Environment Chambers (OPECs)

For the second experiment, outdoor-plant environment chambers (OPECs) [43], covered with Teflon and designed for closed air circulation were used. Air was pumped through an inlet duct in the one side of each chamber, where it was mixed with moisture released from pressure sprinklers. The air was directed upward to avoid exerting pressure on the plants from the side, and to allow more air mixing at the top of the chamber. The air was recycled through the outlet duct on the opposite side of the chamber. The air entering the chambers was adjusted to the set temperature and then passed through an activated charcoal filter to remove ambient O<sub>3</sub>. The control chambers were provided with that ozone-free air. For the O<sub>3</sub>-exposure chambers, the filtered air was enriched with O<sub>3</sub>, the level of which was electronically monitored and controlled.

### 2.2. Plant Materials

In the CSTR study, seven genotypes were tested in our RnUS. The genotypes and their USDA-National Plant Germplasm System accession number or references were “Chinese Spring” [50], “Line E” [51], “Little Club” (Citr 4066), “LMPG 6” [52], “McNair 701” [53], “Morocco” (PI 431591), and “Rusty” (PI 639869). Seeds of the seven genotypes were obtained from the USDA Cereal Disease Lab in Minneapolis, MN, USA. An additional seed source for Chinese Spring was obtained from the USDA-ARS National Small Grains Collection in Aberdeen, ID, USA. Because the two sources of Chinese Spring resulted in near-identical responses in the two experiments, the data of the two sources were combined prior to

the statistical analysis. In the second experiment conducted in OPEC exposure system, the cultivar “Thatcher” (Citr 10003) was additionally included as the eighth genotype. Thatcher was not tested in the CSTR as it was not available at the time of the experiment. The list of tested genotypes could have been extended to include additional genotypes, such as Avocet, however, this genotype was not available at the time of the study.

For both exposure systems, seeds were planted in 170 mL plastic cone-shaped containers (20.7 cm length, 4 and 2.5 cm diameter at the top and the bottom, respectively) filled with Fafard #2 Pro Mix (Fafard, Anderson, SC, USA). Plants were watered from the bottom by placing containers in a 3–5 cm water basin. Water-soluble fertilizer (20-10-20 NPK) was applied to the water basin once a week. Seedlings were grown in CF air ( $O_3$  concentration <10 ppb) in the greenhouse for 30 days after planting. Plants at Zadoks decimal growth stage of 21–23 [54], with the main stem and two tillers, were selected and the fourth leaf on the main stem was tagged before moving the plants to CSTRs or OPECs.

### 2.3. Ozone Treatment and Experimental Design

After being moved to the exposure systems, plants were acclimated for two days in CF air before treated with  $O_3$ . In the CSTRs, a steady-state exposure regime of five  $O_3$  treatments (CF, 50, 70, 90, and 110 ppb) were applied 7 h/day for 5 days at 25 °C and 60% RH, according to the scheme shown in (Figure 1). The actual achieved 7-h treatment averages were 5, 49, 70, 92, and 107 ppb, respectively. The experimental design involved 15 chambers in three blocks. Each treatment was randomly assigned to one chamber per block. One plant per genotype per chamber was treated.  $O_3$  treatments were selected to resemble pre-historic (CF), near-ambient (50 ppb), high 12 h daytime-average (70 ppb), and high hourly-average (90 ppb) and acute instantaneous peaks (110 ppb) observed at a typical sub-urban location in Raleigh NC, USA, during wheat active growing season (March–May), where the 12 h average of the three months over eight years (2006–2008, 2010–2011, and 2013–2015) was 43.82 ppb [55].

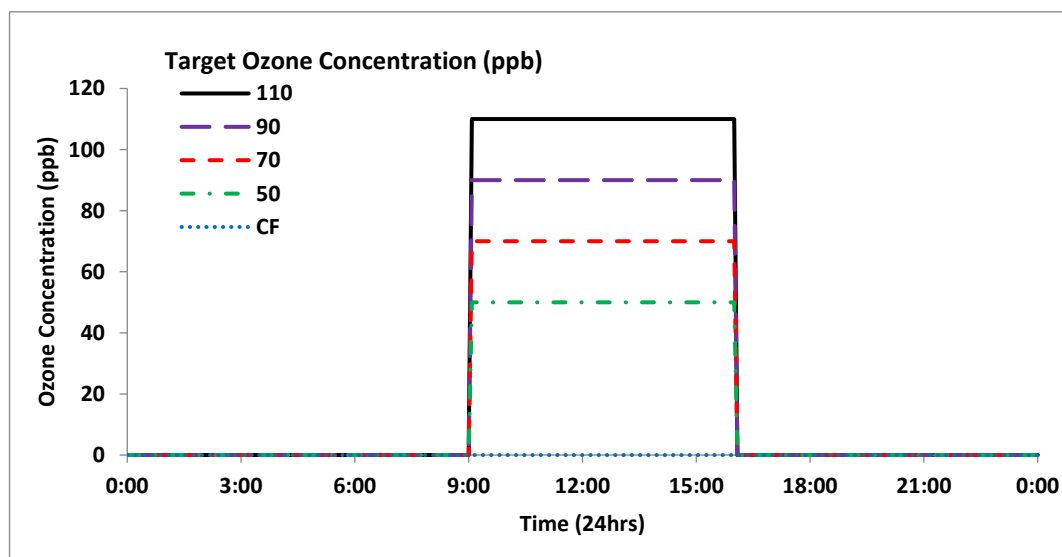


**Figure 1.** Steady-state  $O_3$  treatment regime targeted in continuous stirred tank reactors (CSTRs). The actual achieved treatments were 5, 49, 70, 92, and 107 ppb, respectively.

In the OPECs, plants were exposed for 14 days to one of four  $O_3$  treatments (CF, 50, 70, 90 ppb), using a predefined diurnal  $O_3$  profile of 12 h average of 24 h diurnal profile, at 25/16 °C day/night and 50% RH, as shown in (Figure 2) The actual achieved 12-h treatment averages were 5, 46, 65, and 84 ppb, respectively. The experimental design included eight OPECs, divided into two blocks, four chambers each. Treatments were randomly assigned to one OPEC per block. Two plants per genotype were randomized to each OPEC. The exposure endpoint was determined when  $O_3$  symptoms on the leaves

to be scored of sensitive genotypes were approaching 100% under the highest O<sub>3</sub> treatment (i.e., 110 ppb for CSTRs, and 90 ppb for OPECs).

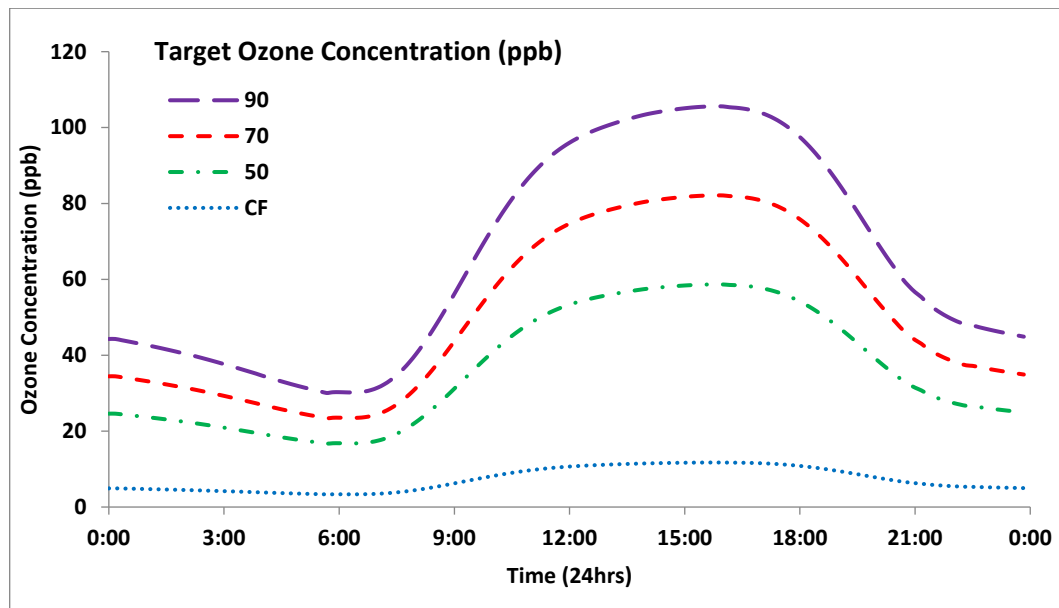


**Figure 2.** Smooth predefined diurnal profiles targeted as O<sub>3</sub> exposure regime in outdoor plant environment chambers (OPECs). The actual achieved treatments were 5, 46, 65, and 84 ppb, respectively.

#### 2.4. Effects of O<sub>3</sub> on Growth Rate

Biomass data collection was not attempted in the CSTR experiment because of the short duration of exposure (5 days). In the OPECs, shoot dry weights were obtained before O<sub>3</sub> treatment (DW1) for three plants per genotype and after treatments (DW2) for all treated plants, by drying samples in paper bags to constant weight under forced air (55 °C). The following dry matter parameters were calculated:

- Dry Matter Accumulation Rate (DMAR)

$$\text{DMAR (g/day)} = \frac{\text{DW2} - \text{DW1}}{t_2 - t_1}$$

whereas  $t_2 - t_1$  is the total exposure period of 14 days.

- Relative Growth Rate (RGR)

$$\text{RGR (\%)} = \frac{\text{Ln}(\text{DW2}) - \text{Ln}(\text{DW1})}{t_2 - t_1}$$

whereas  $t_2 - t_1$  is the total exposure period of 14 days.

- Percent Relative Growth Rate (PRGR)

$$\text{PRGR (\%)} = \frac{\text{RGR under Ozone treatment}}{\text{Average RGR under CF}} \times 100$$

##### 2.4.1. Initial Dry Weight Uniformity and Its Impact on DMAR

Data of initial dry weight (DW1) were checked for inherited differences in biomass between genotypes, then, the regression lines of the DMAR vs. DW1 was plotted to test the hypothesis that initial dry weight might differentially affect the dry matter accumulation rate under different O<sub>3</sub> treatments.

#### 2.4.2. Effects of O<sub>3</sub> Stress on PRGR

The effect of O<sub>3</sub> treatments on the percent relative growth rate (PRGR) was investigated for the tested RnUS wheat genotypes. PRGR values of each genotype were averaged per plot and plotted against the actual treatment achieved.

#### 2.5. Ozone Injury Assessment

Two days after the end of exposure, plants in the CSTR experiment were visually assessed for the percentage of O<sub>3</sub> injury on the fourth leaf of the main stem. In the OPECs, all leaves on the main stem of plants were evaluated at the first day after exposure. However, only third, fourth and fifth leaves were considered for statistical analysis, as the first and second leaves showed some evidence of senescence in all treatments, including the CF control. Visual O<sub>3</sub> injury scores were estimated under constant light conditions according to a 0–100% scale that was devised based on the percent of the leaf area exhibiting chlorosis and necrosis. This scoring guide was established by scanning detached leaves on a flatbed scanner, and analyzed using Assess 2.2, the APS image analysis software (APS, Saint Paul, MN, USA), as described in [26].

#### 2.6. Relationship between O<sub>3</sub> Visible Injury and Relative Growth Rate Responses

The relationships between PRGR and visible O<sub>3</sub> injury were investigated for the seven bread wheat varieties combined, and each of the eight tested genotypes individually, by plotting PRGR against visible injury scores obtained from each plant. Because the CF plants were asymptomatic, their data were excluded for this parameter.

#### 2.7. Statistical Analysis

Glimmix procedure in SAS 9.4 (SAS Inc., Cary, NC, USA) used to analyze the data of the two experiments. CSTRs data were analyzed as a split-plot design, with block random effect. O<sub>3</sub> treatment was placed in the main plot and the genotype in the sub-plot. OPEC data were analyzed as a split-split-plot design with block random effect and sampling, as O<sub>3</sub> treatments were randomly assigned to main plot, with genotypes in the sub-plot and leaf-order in the sub-sub-plot. For both experiments, averages were separated according to Tukey-Kramer's adjustment for multiple comparisons at  $\alpha = 0.05$ .

### 3. Results

#### 3.1. Ozone Injury

All tested genotypes showed the typical O<sub>3</sub> symptoms, starting at the leaf blade tips of the older leaves, in the lower canopy, that expanded towards the younger tissue at the base of the leaf blade. Lower injury levels are mainly flecking. Highly injured leaves were mainly chlorotic at 50 ppb, whereas leaf necrosis became more dominant with the increase in O<sub>3</sub> concentration (Figure A1). The magnitude of symptoms significantly varied among tested genotypes (genotype main effect), with significant first-order interactions in each of the two experiments, except for O<sub>3</sub> interaction with leaf-order in OPECs. In addition, there was a significant second-order interaction (among O<sub>3</sub>, genotype and leaf-order) in the OPEC experiment.

##### 3.1.1. Main Effects of Tested O<sub>3</sub> Treatments on O<sub>3</sub> Injury

To investigate the suitability of the tested O<sub>3</sub> levels, the O<sub>3</sub> injury of all RnUS wheat genotypes were averaged and compared within each experiment (Figure 3). The average O<sub>3</sub> injury varied significantly among O<sub>3</sub> levels within each experiment. However, in CSTRs, there were no significant difference between the 90 and 110 ppb treatments. Therefore, the highest O<sub>3</sub> level was not tested in the OPEC experiment.

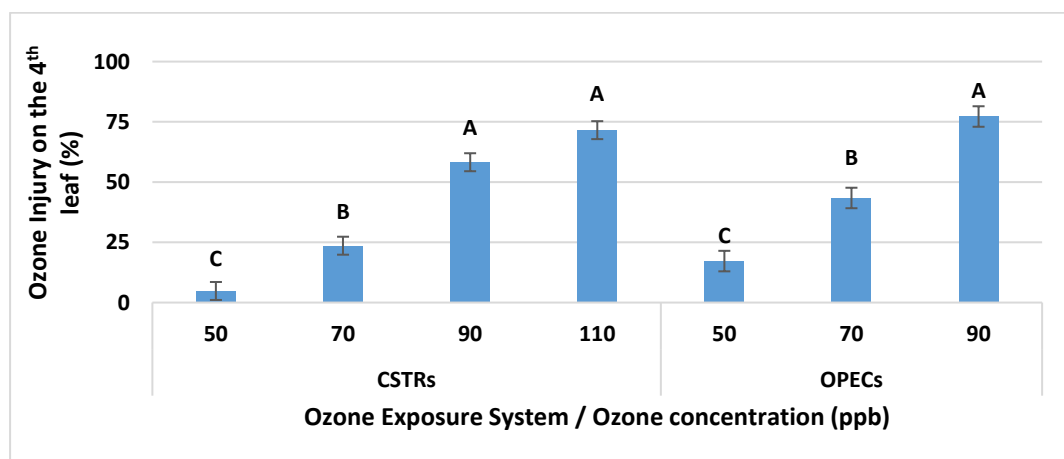


**Figure 3.** The overall average ( $\pm$ SE) of ozone injury of eight rust near-universal susceptible (RnUS) wheat genotypes, under different  $O_3$  levels, for different exposure periods, in two different systems: continuous stirred tank reactors (CSTRs) and outdoor plant environment chambers (OPECs). Means within each exposure system were statistically separated using Tukey-Kramer adjustment for multiple comparisons. Means marked with the same letter are not significantly different at  $\alpha = 0.05$ .

### 3.1.2. Genotype Main Effects and Overall Ranking of the Genotypes According to Their $O_3$ Injury Responses

According to the average  $O_3$  injury in each experiment, the RnUS wheat genotypes showed a consistent overall sensitivity ranking in the two experiments. Under short-term exposure in CSTRs, the bread wheat genotype Chinese Spring was found to be  $O_3$ -tolerant, whereas LMPG 6 was considered  $O_3$  sensitive, as shown in (Figure 4). The other genotypes had moderate  $O_3$  injury, compared to the sensitive and tolerant genotypes. Similarly, the extended exposure in the second OPEC experiment resulted in identical genotype ranking, but with more refined separation among the tested genotypes. Thatcher was found to be the most sensitive RnUS genotype in OPECs, as shown in (Figure 5).

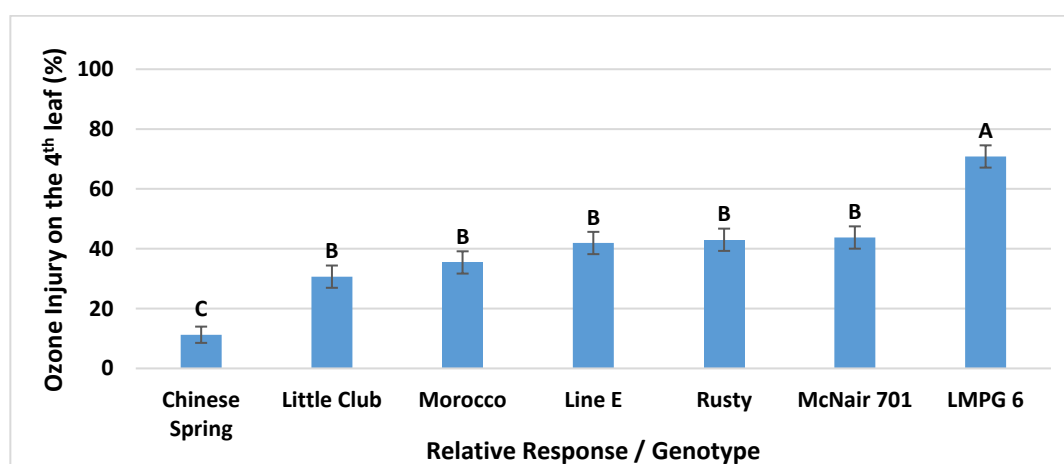


**Figure 4.** The overall average ( $\pm$ SE)  $O_3$  injury on the fourth leaf of rust near-universal susceptible genotypes, after exposure to four different  $O_3$  levels (50, 70, 90, 110 ppb), for 5 days (7 h/day), at 25 °C and 60% RH, in continuous stirred tank reactors (CSTRs). Injury were visually estimated two days after the end of exposure, under constant light conditions according to a 0–100% scale. Means were statistically separated using Tukey-Kramer adjustment for multiple comparisons. Means marked with the same letter are not significantly different at  $\alpha = 0.05$ .

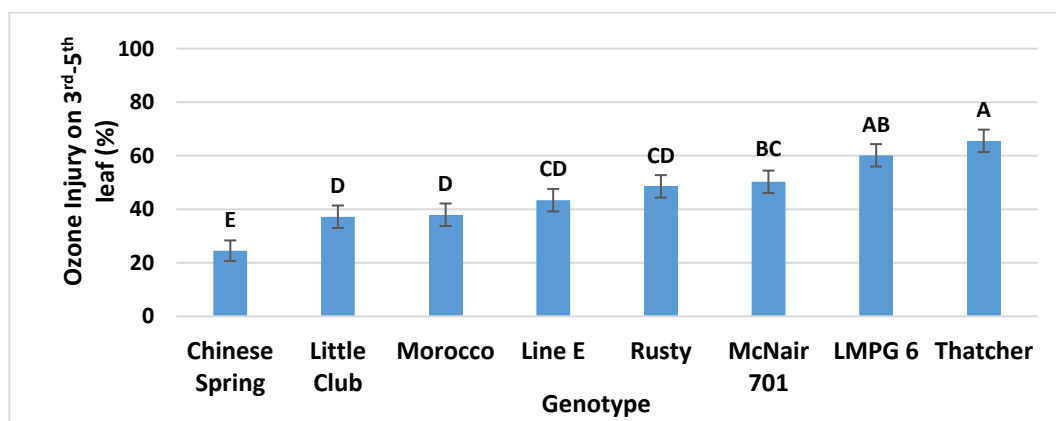


**Figure 5.** The overall average O<sub>3</sub> injury (on the third–fifth leaf) of rust near-universal susceptible genotypes, after exposure to three different O<sub>3</sub> levels (50, 70, 90 ppb) for 14 days (12 h/day), at 25 °C and 50% RH, in OPECs. Injury was visually estimated, under constant light conditions according to a 0–100% scale. Values are means (±SE) statistically separated using Tukey-Kramer adjustment for multiple comparisons. Means marked with the same letter are not significantly different at  $\alpha = 0.05$ .

### 3.1.3. Interaction between O<sub>3</sub> Level and Genotype

#### Interaction of O<sub>3</sub> Level and Genotype on O<sub>3</sub> Injury in CSTRs

Elevated O<sub>3</sub> injury data in CSTRs showed a significant interaction between genotypes and O<sub>3</sub> treatments. At the O<sub>3</sub> exposure levels of 50 ppb, there were no significant differences in visual injury between the genotypes, as shown in (Figure 6). However, when the genotypes were compared at 70 ppb of O<sub>3</sub>, LMPG 6 showed significantly greater injury than the other tested genotypes. Chinese Spring and Little Club had significantly less O<sub>3</sub> injury than LMPG 6 at 90 ppb. At the highest exposure level of 110 ppb of O<sub>3</sub>, Chinese Spring showed the least amount of O<sub>3</sub> injury. In comparing the O<sub>3</sub> concentrations within each genotype, Chinese Spring showed no significant difference in foliar injury from 50 ppb (1%) to 110 ppb (21%). LMPG 6 was the only genotype that had significantly greater injury at 70 ppb compared to 50 ppb, with no significant differences among the three greatest concentrations. McNair-701 and Little Club showed a gradient in O<sub>3</sub> responses, whereas Morocco, Line E, Rusty showed differences between the two lowest and the two greatest concentration, as shown in (Figure 6).

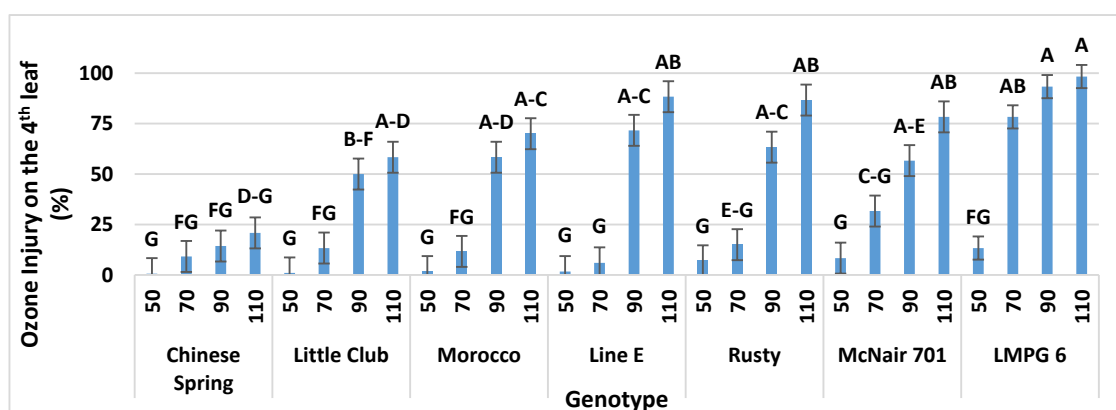


**Figure 6.** Effect of four different O<sub>3</sub> levels (50, 70, 90, and 110 ppb) on O<sub>3</sub> injury on the fourth leaf of rust near-universal susceptible genotypes, exposed for 5 days (7 h/day), at 25 °C and 60% RH, in CSTRs. Injury were visually estimated, under constant light conditions according to a 0–100% scale. Values are means (±SE) statistically separated using Tukey-Kramer adjustment for multiple comparisons. Means marked with the same letter are not significantly different at  $\alpha = 0.05$ .

### Interaction of O<sub>3</sub> Level and Genotype on O<sub>3</sub> Injury in OPECs

In the OPECs, genotypes were exposed at four O<sub>3</sub> concentrations, CF, 50, 70, and 90 ppb. At an exposure of 50 ppb, Thatcher and LMPG 6 had significantly greater O<sub>3</sub> injury than the other genotypes (Figure 7). At 70 ppb, these two sensitive genotypes had significantly more O<sub>3</sub> injury than Chinese Spring (14%) and Little Club (34%), as the other genotypes showed intermediate responses. When exposed to 90 ppb O<sub>3</sub>, only Chinese Spring had significantly less O<sub>3</sub> injury than Rusty, McNair 701, LMPG 6, and Thatcher, while Little Club, Morocco, and Line-E had intermediate injury levels.

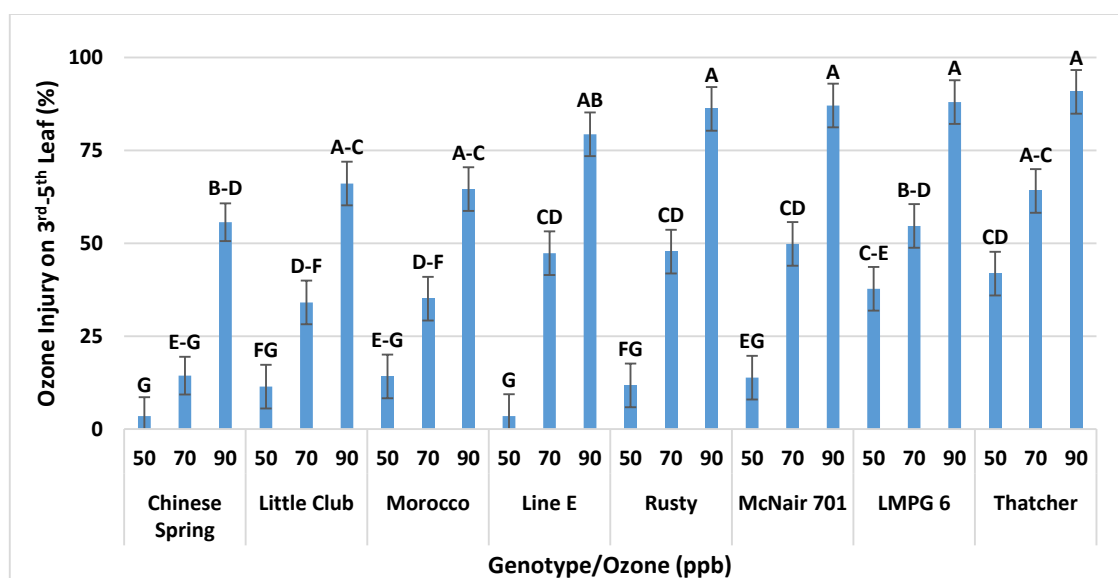


**Figure 7.** Average ( $\pm$ SE) O<sub>3</sub> injury (on the third–fifth leaf) of rust near-universal susceptible genotypes, at three different O<sub>3</sub> levels, exposed for 14 days (12 h/day), at 25 °C and 50% RH, in OPECs. Injury was visually estimated, under constant light conditions according to a 0–100% scale. Means were statistically separated using Tukey-Kramer adjustment for multiple comparisons. Means marked with the same letter are not significantly different at  $\alpha = 0.05$ .

When comparing concentrations effects within genotypes in OPECs, all tested genotypes, except for Thatcher, showed statistically significant greater percentages of O<sub>3</sub> injury at 90 ppb compared to 70 ppb. However, when comparing O<sub>3</sub> injury at 70 ppb to 50 ppb, genotypes can be placed into one of three categories: (1) sensitive genotypes (i.e., Thatcher and LMPG 6) showed relatively high O<sub>3</sub> injury at both concentrations that were not statistically different from one another, due to high injury levels at 50 ppb; (2) genotypes of intermediate sensitivity (McNair 701, Rusty, Line E) showed significant differences among three concentrations, as O<sub>3</sub> injury at 50 ppb were significantly less than 70 ppb; and (3) tolerant genotypes (Morocco, Little Club, and Chinese Spring) that had relatively low injuries at both 50 and 70 ppb that were not significantly different from one another, but were significantly different from injury exhibited after exposure to 90 ppb.

#### 3.1.4. Interaction of Leaf-Order and O<sub>3</sub> Level on O<sub>3</sub> Injury

##### Interaction of Leaf-Order and O<sub>3</sub> Level on O<sub>3</sub> Visible Injury in OPECs

There was a significant interaction between the leaf-order and O<sub>3</sub> level factors in OPECs ( $p$ -value < 0.0001). The magnitude of O<sub>3</sub> injury on the third and fourth leaf had increased with the increase in O<sub>3</sub> level (Figure 8). The 5th leaf showed significant increase in O<sub>3</sub> injury only at 90 ppb. At 50 ppb, the third leaf showed more injury than the fourth and fifth leaves, while at 70 ppb, all three leaves were significantly different from each other. The fifth leaf showed significantly less symptoms than the lower leaves at 90 ppb.

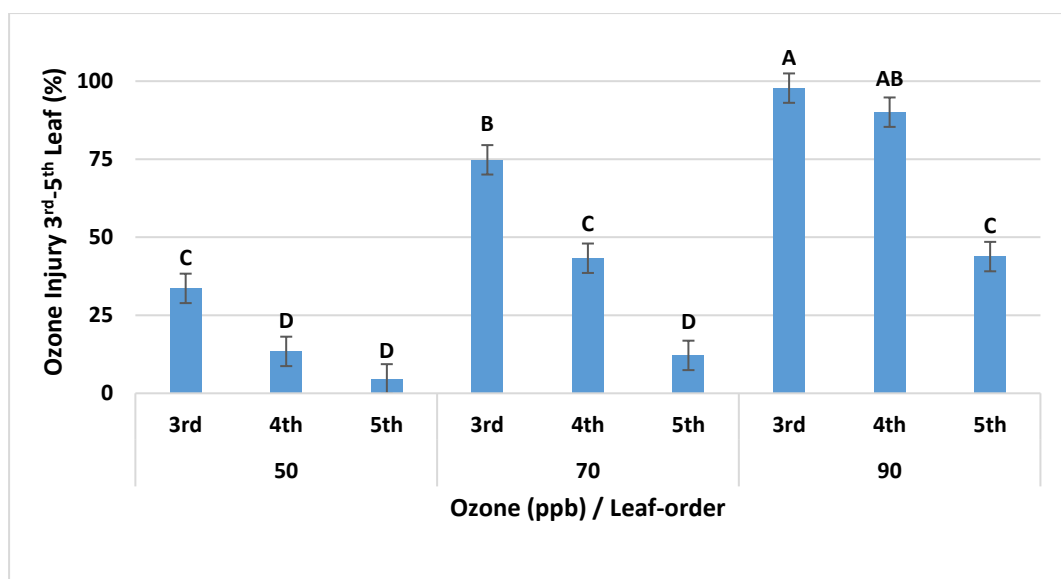


**Figure 8.** Interplay of leaf-order and O<sub>3</sub> treatment on average O<sub>3</sub> injury (±SE) on the third–fifth leaf of rust near-universal susceptible genotypes, exposed for 14 days (12 h/day), at 25 °C and 50% RH, in OPECs. Injury was visually estimated, under constant light conditions on a 0–100% scale. Values are means (±SE) statistically separated using Tukey-Kramer adjustment for multiple comparisons. Means marked with the same letter are not significantly different at  $\alpha = 0.05$ .

### 3.1.5. Interaction of Leaf-Order and Genotype on O<sub>3</sub> Injury in OPECs

There was no significant interaction between the leaf-order and genotype factors in OPECs ( $p$ -value = 0.4059). Older leaves of all genotypes were more sensitive than younger ones (Figure 9).

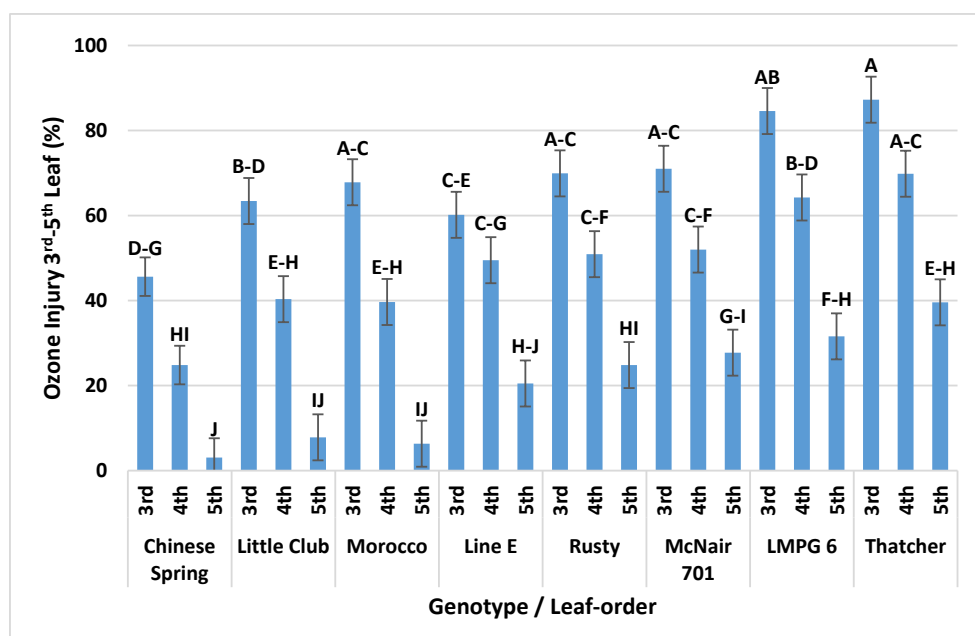


**Figure 9.** Interplay of leaf-order (third–fifth leaf) and genotype on average O<sub>3</sub> injury (±SE) of rust near-universal susceptible genotypes, exposed to O<sub>3</sub> (50, 70, 90 ppb) for 14 days (12 h/day), at 25 °C and 50% RH, in OPECs. Injury was visually estimated, under constant light conditions on a 0–100% scale. Values are means (±SE) statistically separated using Tukey-Kramer adjustment for multiple comparisons. Means marked with the same letter are not significantly different at  $\alpha = 0.05$ .

### 3.1.6. Interaction of Leaf-Order, O<sub>3</sub> Levels and Genotype (2nd-Order Interaction) on O<sub>3</sub> Injury in OPECs

There was a significant second-order interaction between the leaf-order, O<sub>3</sub> level, and genotype factors in OPECs ( $p$ -value < 0.0001). At the lower O<sub>3</sub> concentration, differences among genotypes were mainly derived by O<sub>3</sub> injury on third leaves, with less pronounced differences on fourth and fifth leaves (Figure 10). In contrast, at the 90 ppb O<sub>3</sub> level, differences among the fifth leaves were more pronounced, because most of the third and fourth leaves were highly injured.

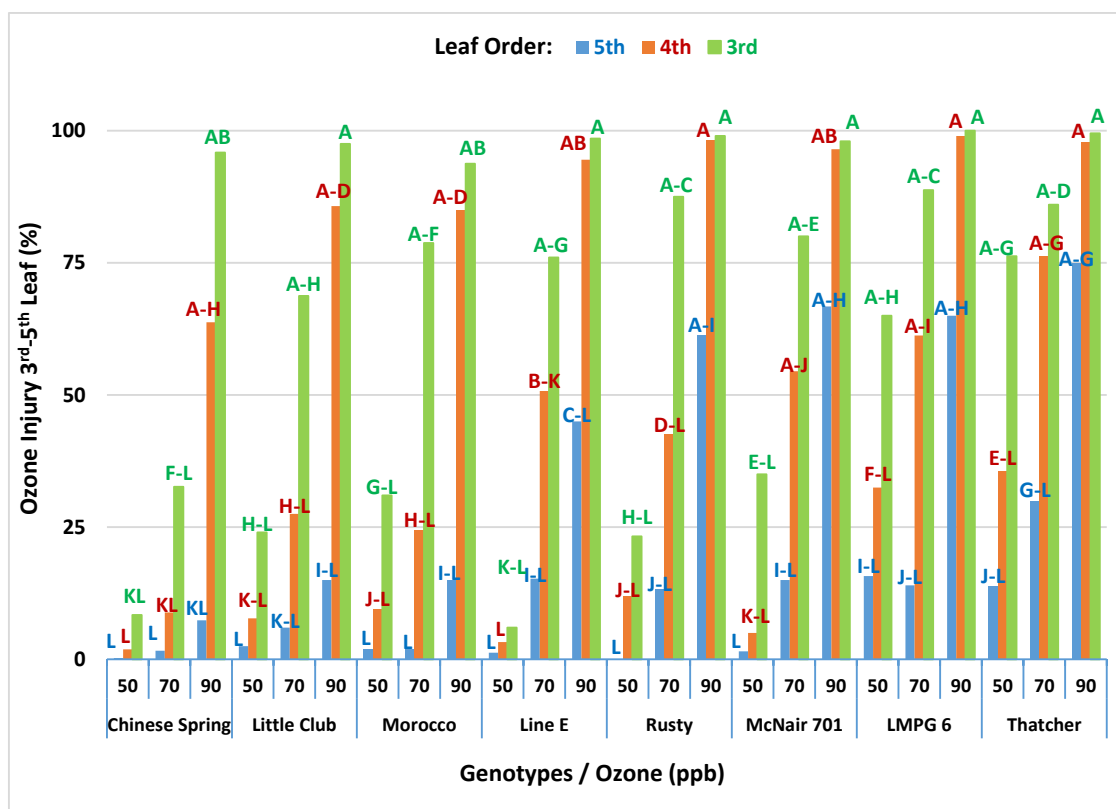


**Figure 10.** O<sub>3</sub> injury on the third–fifth leaf of rust near-universal susceptible genotypes, at three different O<sub>3</sub> levels, exposed for 14 days (12 h/day), at 25 °C and 50% RH, in OPECs. Injury was visually estimated, under constant light conditions according to a 0–100% scale. Means were statistically separated using Tukey-Kramer adjustment for multiple comparisons. Means marked with the same letter are not significantly different at  $\alpha = 0.05$ .

## 3.2. Dry Matter Accumulation

### 3.2.1. Initial Dry Weight Uniformity and Their Impact on DMAR

Although the genotypes were planted at the same day, and were selected for emergence time and growth stage uniformity, as well as canopy structure, they differed in their initial dry matter prior to the exposure, as shown in Figure 11. When the data of the seven bread-wheat genotypes were combined, the initial dry weight per plant seemed to have a positive effect on the dry matter accumulation rate, as shown in Figure 12. Genotypes with smaller dry weight had lower dry matter accumulation rates than genotypes with greater initial dry weight when compared under the same O<sub>3</sub> treatment. For all plant sizes, DMAR was decreased by increasing O<sub>3</sub> levels.

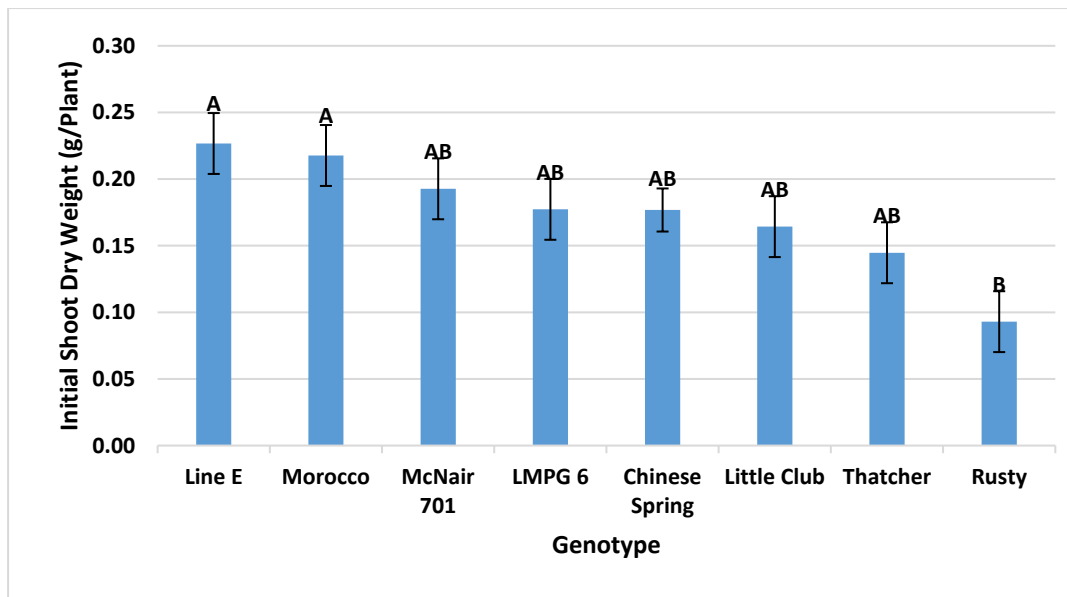


**Figure 11.** The initial dry weight (g) per plant ( $\pm$ SE) of the eight genotypes at 30 days after planting, prior to O<sub>3</sub> treatment in OPECs. Means within each exposure system were statistically separated using Tukey-Kramer adjustment for multiple comparisons. Means marked with the same letter are not significantly different at  $\alpha = 0.05$ .

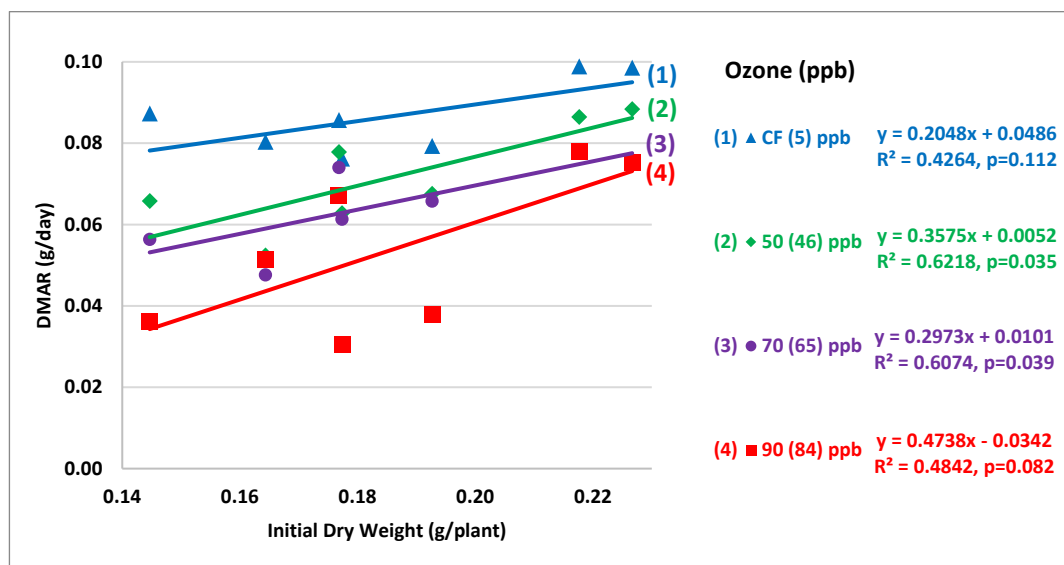


**Figure 12.** The regression line of the dry matter accumulation rate (per plant per day) on the initial weight of the seven bread wheat genotypes under different O<sub>3</sub> treatments (10, 50, 70, and 90 ppb) for 14 days (12 h/day). Actual treatments achieved were 5, 46, 65 and 84, respectively.

### 3.2.2. Effects of O<sub>3</sub> Stress on PRGR

There were significant main effects of both O<sub>3</sub> level and genotype ( $p < 0.0001$ ), and a significant interaction between the two factors ( $p = 0.0143$ ) on PRGR (Figures 13 and 14). Both 50 and 70 ppb treatments resulted in significant reduction in PRGR comparing to CF, with no significant difference between the two treatments. The 90 ppb treatments showed the least PRGR, which was significantly less than 70 ppb (Figure 13A). PRGR of the tested genotypes differentially responded to the tested O<sub>3</sub> treatments (Figure 13B). Chinese Spring was the most tolerant genotype; Rusty was the most sensitive, whereas the rest of the tested genotypes were intermediate.

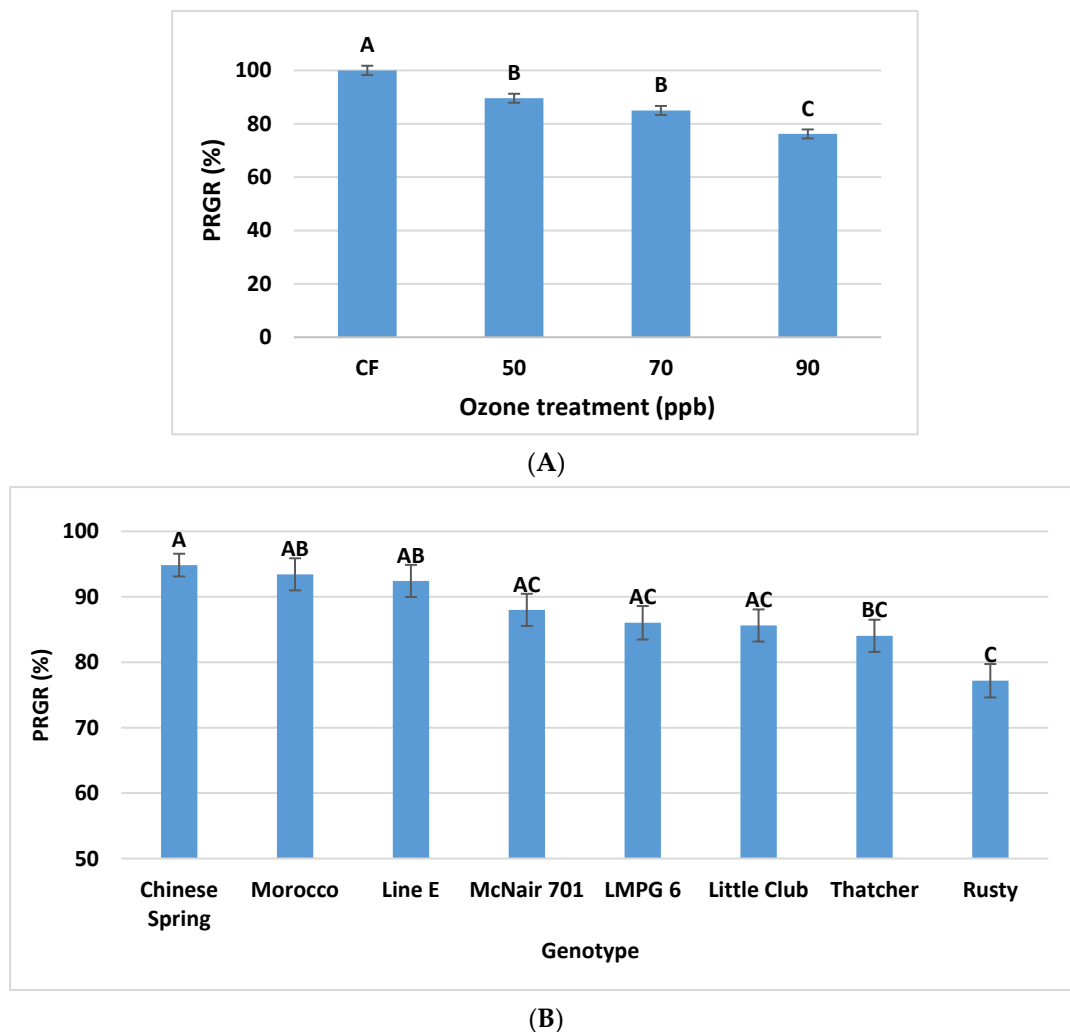
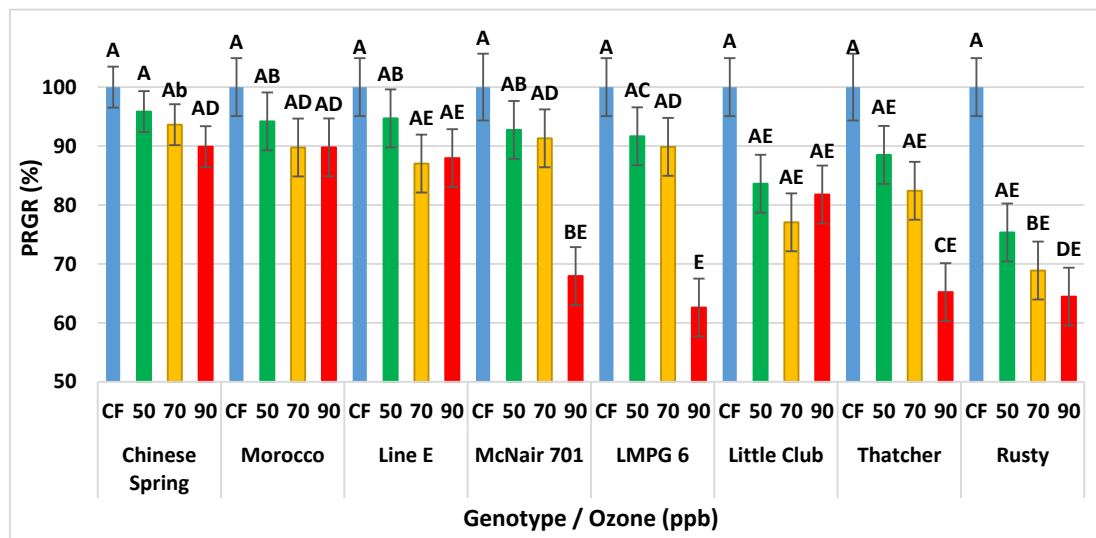


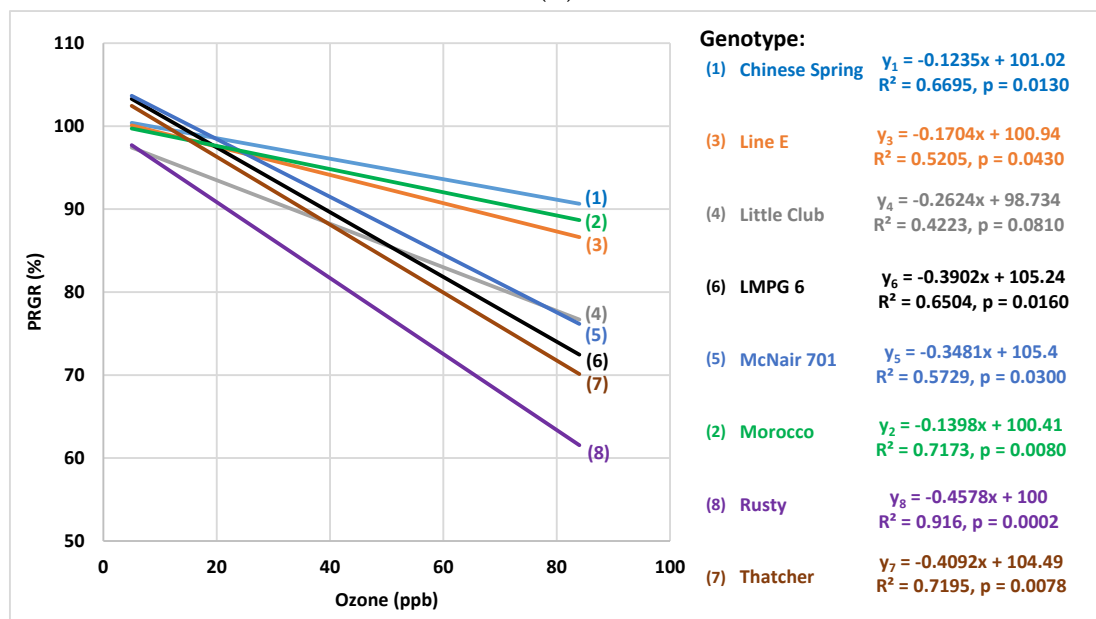
**Figure 13.** Percent relative growth rate [relative dry matter accumulation rate (RDMAR) under O<sub>3</sub> treatment, referenced to the RDMAR in charcoal-filtered air (O<sub>3</sub> = 5 ppb)], of eight rust near-universal susceptible genotypes and their trends in response to different O<sub>3</sub> levels of CF, 50 70 and 90 ppb (actual achieved treatments were 5, 46, 65, and 84 ppb, respectively) for 14 days (12 h/day), in OPECs (at 25 °C and 50% RH): (A) O<sub>3</sub> main effect; (B) genotype main effect. Values are means ( $\pm$ SE) statistically separated using Tukey-Kramer adjustment for multiple comparisons. Means marked with the same letter are not significantly different at  $\alpha = 0.05$ .

There was a significant reduction in the PRGR with increasing O<sub>3</sub> concentrations for all the genotypes, as compared to charcoal filtered air. However, the genotypes showed different trends in their biomass response to O<sub>3</sub> stress. The bread wheat genotypes could be classified into three groups. The first group included Chinese Spring, Morocco, and Line E. Genotypes of this group showed reduced O<sub>3</sub> impacts on biomass production and less reduction in PRGR at the three O<sub>3</sub> concentrations tested, as evident in the lack of significant difference among O<sub>3</sub> treatments with each genotype Figure 14A and small slope value of the trend lines Figure 14B. The second group of bread wheat included only Little Club. This genotype was similar to the first group in the lack of significance difference among O<sub>3</sub> treatments (Figure 14A), however, it had larger slope value of the regression line (Figure 14B). Additionally, it was the only genotype with non-significant regression line ( $p = 0.0810$ ). The third group included McNair 701, LMPG 6, and Thatcher. These genotypes were more sensitive than the first group, especially at 90 ppb (Figure 14A), and showed steeper regression lines (Figure 14B). On the other hand, the durum wheat genotype Rusty was the most sensitive genotype in terms of biomass

response to O<sub>3</sub> stress. Rusty showed overall 0.46% reduction in RGR for every 1 ppb increase in O<sub>3</sub> concentration. Additionally, it was the only genotype with significant difference at 50(46) ppb.



(A)



(B)

**Figure 14.** Percent relative growth rate (PRGR) [relative dry matter accumulation rate (RDMAR) under O<sub>3</sub> treatment referenced to their RDMAR in charcoal-filtered air (CF)], of eight rust near-universal susceptible genotypes at different O<sub>3</sub> levels of 50, 70, 90 ppb (actual achieved were 5, 46, 65, and 84 ppb, respectively) for 14 days (12 h/day), in OPECs (at 25 °C and 50% RH): (A) Interaction of genotype and O<sub>3</sub> concentration on PRGR, values are means (±SE) statistically separated using Tukey-Kramer adjustment for multiple comparisons, and means marked with the same letter are not significantly different at α = 0.05; (B) PRGR regression lines on O<sub>3</sub> concentration.

### 3.2.3. Relationship between Visible Injury and Relative Growth Rate Responses of RnUS Wheat Genotypes to O<sub>3</sub> Stress

When PRGR data of the seven bread RnUS wheat genotypes were combined (after excluding the CF treatment) and plotted against the observed O<sub>3</sub> injury (Figure 15), a negative correlation

was observed, with a 96.6% interception, and a negative slope of  $-0.23$ , suggesting a non-threshold relationship between visible  $O_3$  injury and relative growth rate responses of these RnUS genotypes.

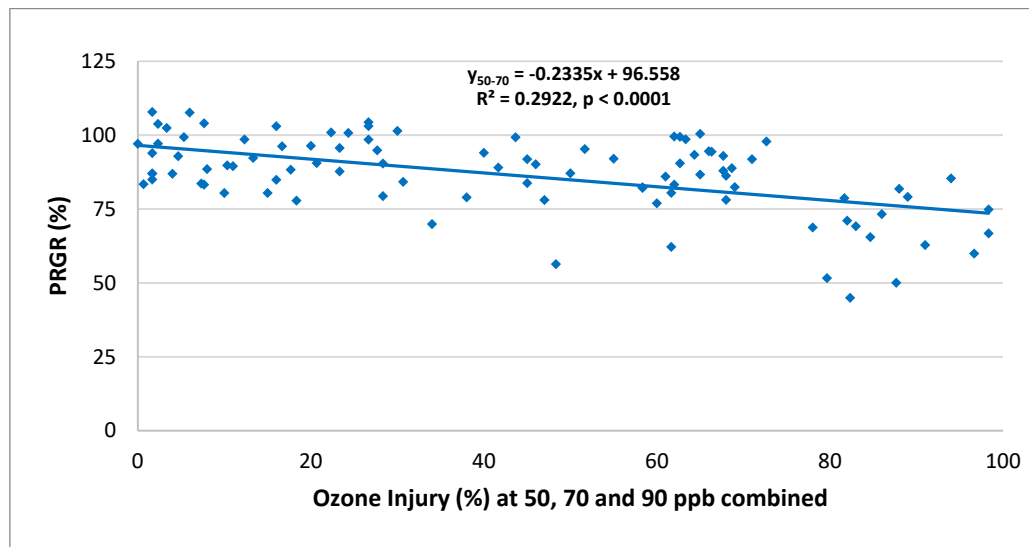


**Figure 15.** General relationship between percent relative growth rate (PRGR) and  $O_3$  injury on third–fifth leaves of seven rust near-universal susceptible genotypes of bread wheat after exposure to different  $O_3$  levels (50, 70, 90 ppb) for 14 days (12 h/day), in OPECs (at 25 °C and 50% RH). PRGR is the relative growth rate of individual plants referenced to the genotype’s average RGR in charcoal-filtered air ( $O_3 = 5$  ppb).

By considering the effect of the different elevated  $O_3$  levels separately (Figure 16), it was clear that  $O_3$  symptoms observed at 50 ppb were not correlated with the corresponding PRGR ( $p = 0.719$ ; both  $R^2$  and the slope were nearly zero). At 70 ppb, there were significant ( $p = 0.0099$ ) and stronger negative relationship ( $R^2 = 0.20$ ), and the slope was greater ( $-0.23$ ). This significant trend continued at 90 ppb ( $p = 0.0012$ ) with the strongest negative relationship ( $R^2 = 0.20$ ) and the greatest slope ( $-0.30$ ).

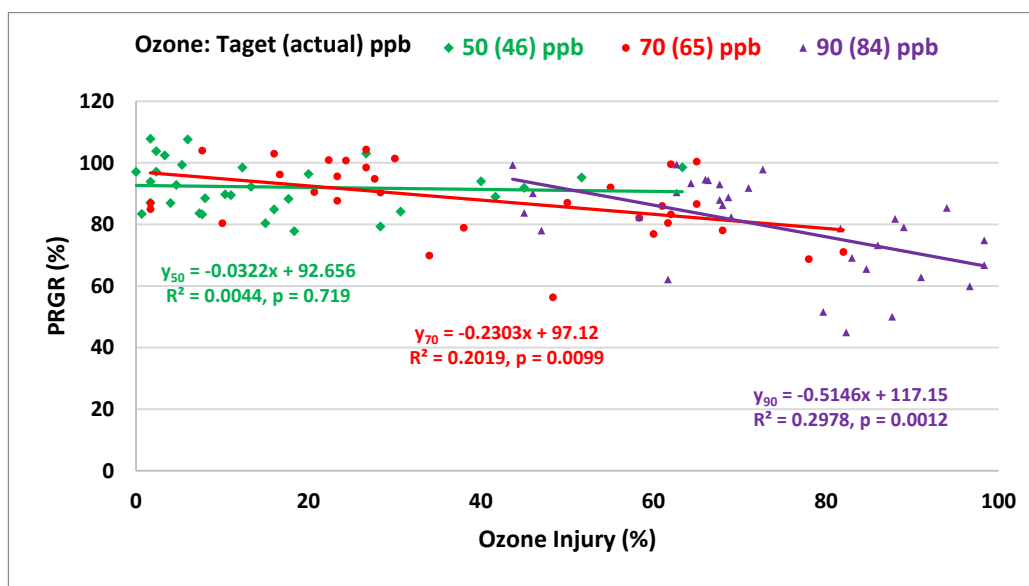


**Figure 16.** Relationship between percent relative growth rate (PRGR) and  $O_3$  injury on third–fifth leaves of seven RnUS wheat genotypes at each of three different  $O_3$  levels of 50, 70, and 90 ppb (12 h/day, at 25 °C and 50% RH, for 14 days in OPECs). PRGR is the relative growth rate of individual plants referenced to the genotype’s average RGR in charcoal-filtered air ( $O_3 = 5$  ppb).

When data of the different RnUS wheat genotypes were plotted individually (Figure 17), the tolerant genotype Chinese Spring had the least slope ( $-0.0618$ ) and  $R^2$  value ( $0.0328$ ), indicating that  $O_3$  injury on plants is not correlated ( $p = 0.397$ ) with  $O_3$  impacts on biomass production. On the other hand, bread wheat varieties that were ranked sensitive to  $O_3$  injury (McNair-701, LMBG-6, and Thatcher) showed the greater slope ( $-0.31$ ,  $-0.38$ , and  $-0.33$ , respectively), stronger correlations ( $p = 0.036$ ,  $0.0036$ , and  $0.057$ ) and  $R^2$  values ( $0.30$ ,  $0.47$ , and  $0.35$ , respectively), indicating stronger correlation between PRGR and  $O_3$  symptoms. Interestingly, Little Club had the least values for the intercept ( $85.8\%$ ) among the bread wheat genotypes. The durum wheat Rusty had the least values for the intercept ( $74.8\%$ ) among all tested genotypes, and a slope value of  $-0.11$ .

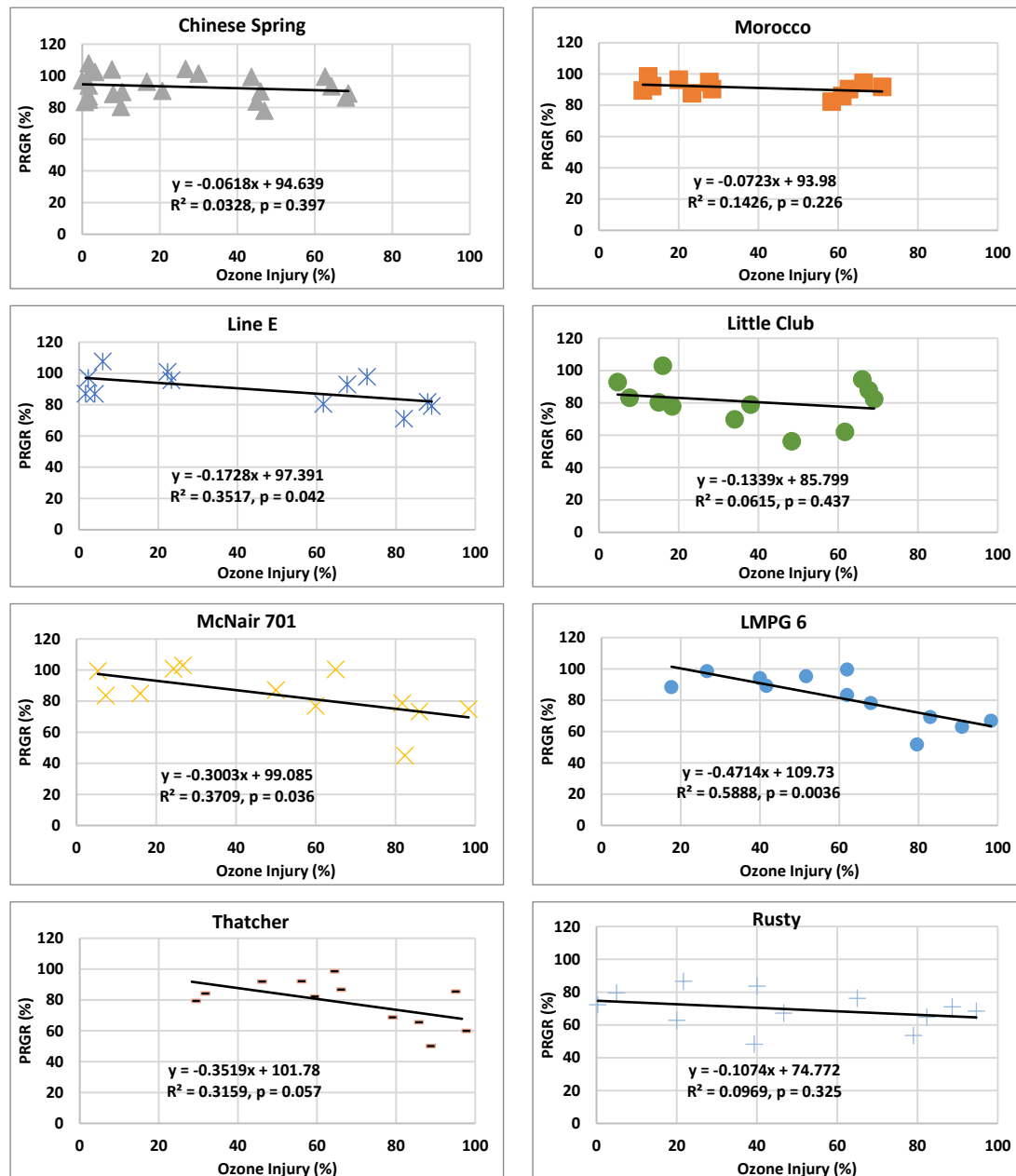


**Figure 17.** Relationship between percent relative growth rate (PRGR) and  $O_3$  injury on third–fifth leaves of each of the eight rust near-universal susceptible genotypes at three different  $O_3$  levels of 50, 70, and 90 ppb (12 h/day, at 25 °C and 50% RH, for 14 days in OPECs). PRGR is the percentage of RGR of each plant referenced to the genotype’s average RGR in charcoal-filtered air ( $O_3 = 5$  ppb).

#### 4. Discussion

Using visible symptoms and relative growth rate, the results of this study showed that plants, and leaves at different leaf order (on the main stem), of the eight rust near-universal susceptible (RnUS) wheat genotypes differentially responded to O<sub>3</sub> exposure. The RnUS wheat genotypes are a diverse group [3–6]; they differ in their genetic background, the date of development or release, the reason for their development (varieties vs. test lines), their vernalization requirement (spring vs. winter wheat) and the species (bread vs. durum wheat) [6]. The observed RnUS responses to O<sub>3</sub> stress are consistent with differential O<sub>3</sub> responses reported among diverse groups of wheat species and varieties [40,44,56,57]. These differential responses make RnUS suitable for identifying O<sub>3</sub> tolerance among breeding materials, and for simultaneous breeding of resilient varieties bearing O<sub>3</sub> tolerance and rust resistance, as well as investigating the sub-canopy interplay of O<sub>3</sub> stress, wheat genotype, and pathogens, including wheat rusts.

O<sub>3</sub> is known to cause a continuum of two phases: sub-symptomatic and visible symptom responses. The ratio between the two phases on plants depends on the genotype's sensitivity, the O<sub>3</sub> level and the duration of exposure [23–26]. In this study, we focused on the O<sub>3</sub> visible symptoms observed under O<sub>3</sub> levels ranging from 50–100 ppb, which identify wheat sensitivity in level mimicking current and future O<sub>3</sub> levels, and help to understand the reported O<sub>3</sub> conducive impacts on necrotrophic pathogens, and negative impacts on biotrophic pathogen like rusts [1,58–63]. Rust pathogens require living tissue, and visible O<sub>3</sub> injury at different leaf order in the canopy suggests a gradient of reduction in plant tissue available for these pathogens to infect.

Interestingly, the tested RnUS genotypes maintained a consistent relative sensitivity/tolerance ranking for visible injury in the two O<sub>3</sub> exposure systems (i.e., CSTRs and OPECs), despite the differences in exposure concentration, duration, regime, and environmental conditions, in addition to the difference in the order of scored leaves (fourth vs. third–fifth leaf in CSTRs and OPECs, respectively). Overall, LMPG 6 and Thatcher were O<sub>3</sub> sensitive, in contrast to Chinese Spring which was found to be O<sub>3</sub> tolerant. The other five genotypes had moderate O<sub>3</sub> injury. This consistency might be due to the use of a suitable ending point, by terminating the exposure when O<sub>3</sub> symptoms on the most sensitive tested genotype was approaching 100%, under the highest O<sub>3</sub> concentration. Scoring plants at such a standard ending point for screening experiments would allow for the maximum symptoms on the tolerant varieties without over-exposing sensitive ones. Hence, the results obtained under different conditions would be comparable, especially if reference-tolerant (e.g., Chinese Spring) and sensitive (Thatcher) genotypes were universally used. Because of their universal use worldwide [6], RnUS genotypes could be ideal reference material in O<sub>3</sub> screenings.

The biomass data showed poor correlations between visible symptoms and PRGR in tolerant genotypes, which suggest that these genotypes can maintain high efficiency of their photosynthetic machinery, possibly in younger leaves where symptoms were not observed. On the other hand, sensitive varieties suffered from O<sub>3</sub> symptoms on both lower and upper canopy, leaving less unimpaired photosynthetic tissue to contribute to biomass production. Moreover, the intercept values of Little Club and Rusty were 85.8 and 74.8%, respectively. These intercept values are evidence of compromised growth in the absence of visible symptoms, as the two genotypes might undergo 14.2 and 25.2% loss in RGR, respectively, in non-symptomatic plants. This is a clear indication that even in the absence of visible symptoms, reduction in the relative growth rate is expected. This suggests that screening based on biomass production under O<sub>3</sub> stress is critical. In the case of Little Club, this reduction could be the result of O<sub>3</sub> avoidance by induced stomatal closure, which might be supported by the narrow range of O<sub>3</sub> injury levels observed, which does not exceed a maximum of 69% on any plant under any treatment. As for Rusty, it is more likely that this reduction in RGR is the result of direct post-entry O<sub>3</sub> impact on photosynthesis, because of the high injury levels observed with a maximum O<sub>3</sub> injury of 94.7%. The findings of this study show that visible symptoms could only be used as an indicator for biomass sensitivity under severe O<sub>3</sub> stress (e.g., 90 ppb). At lower O<sub>3</sub> concentrations, it is difficult to differentiate between the tolerant and sensitive varieties if depending solely on visible symptoms.

For screening wheat for O<sub>3</sub> tolerance, visible symptom and relative growth rate responses have different requirements in terms of available resources and time. Selecting against O<sub>3</sub> visible symptoms might be the most feasible approach, however, it does not always reflect the biomass responses. A quantitative trait locus (QTL) for leaf bronzing on chromosome 5A was identified in wheat, yet it was present in most of the tested genotypes, therefore the value in selection for this allele in a breeding program is not clear [44]. Visible symptoms observed in this study were in the form of chlorotic flecking that progresses into chlorosis, rather than leaf bronzing. It would be of interest to assess the role of the leaf bronzing locus in the differential O<sub>3</sub> response of the RnUS. However, both this study and [44] support the use of foliar injury as a tool for high throughput screening.

Trends in PRGR were consistent with visible injury ranking for the tolerant genotype Chinese Spring and two of the moderately sensitive genotypes (Morocco, and Line E), as well as the more sensitive genotypes McNair 701, LMPG 6, and Thatcher (Figure 14). On the other hand, trends of biomass data of Little Club and Rusty seemed different from their injury responses. Little Club seemed to be more sensitive to the presence of O<sub>3</sub> than the concentration, as PRGR dropped with O<sub>3</sub> increase from CF to 50 ppb, with no further decrease in PRGR at the higher O<sub>3</sub> levels, as evident from the small slope values (Figure 14), this might support an O<sub>3</sub>-avoidance mechanism. In contrast, the durum wheat genotype Rusty was the most sensitive genotype in terms of biomass responses (Figure 14). Overall, Rusty was ranked in this study as moderately sensitive to O<sub>3</sub> injury, although durum wheat is presumed more tolerant to O<sub>3</sub> than bread wheat [34]. This level of sensitivity makes Rusty an ideal material for identifying the genetic control of O<sub>3</sub> tolerance in durum wheat. Populations already made of crosses between Rusty and other durum wheat varieties with confirmed O<sub>3</sub> tolerance could be used to map O<sub>3</sub> tolerance. Therefore, further screening of more durum wheat varieties for O<sub>3</sub> tolerance is needed, especially those varieties that were crossed with Rusty to form mapping populations.

The positive correlation between dry matter accumulation, under all O<sub>3</sub> treatments, and the initial dry weight suggests that genotypes with rapid growth (prior to O<sub>3</sub> exposure) at the seedling stage might show less biomass sensitivity to O<sub>3</sub> stress when screened. A standardized high throughput screening of large numbers of genotypes is critical for making progress in breeding for O<sub>3</sub> tolerance. One potential standardization method is to start the exposure shortly after the full development of the second leaf, consequently, minimizing the differences in initial biomass. In addition, early screening will allow for capturing the exponential nature of growth at this early stage, which would maximize the potential for detecting the inherited O<sub>3</sub> tolerance, with minimal environmental interference.

Due to its importance for global food security, wheat is the most studied crop for O<sub>3</sub> responses [56]. However, breeding O<sub>3</sub>-tolerant wheat is yet to be widely conducted. Although differences in O<sub>3</sub> responses were documented among wheat cultivars [21,44], more information on key genetic stocks is critically lacking. Hence, the identification of the O<sub>3</sub> responses of RnUS commonly used as genetic stocks (e.g., Chinese Spring and Thatcher) could have a substantial impact on breeding for O<sub>3</sub> tolerance. For example, Chinese Spring was the most tolerant genotype to both O<sub>3</sub>-induced symptoms and biomass reductions. This variety is central for genetic studies of wheat, consequently, it was selected for obtaining the first whole-genome sequence [64], and is usually used as a parent that lacks many agronomic traits [65]. However, based upon the evidence provided here, Chinese Spring could additionally be used as a source of O<sub>3</sub> tolerance in bread wheat. The wide diversity of available genetic stocks for Chinese Spring [66] makes it ideal for identifying the location of O<sub>3</sub> tolerance in wheat. O<sub>3</sub> tolerance has been attributed to genomes AABB, whereas the sensitivity has been found in genome DD [34]. The availability of 21 monosomic lines in the Chinese Spring background were used to attribute O<sub>3</sub> tolerance to chromosome 7A [26]. Biparental mapping populations of Chinese Spring are suitable for identifying markers associated with this source of O<sub>3</sub> tolerance. For example, a mapping population of Chinese Spring was used for identifying adult plant resistance to leaf rust [5], whereas another mapping population was used to map *Lr34* in a near-isogenic line of the sensitive background genome of Thatcher [67]. These mapping populations could also be used to map O<sub>3</sub> tolerance in Chinese Spring, if phenotyped for O<sub>3</sub> tolerance.

## 5. Conclusions

Increased wheat production is essential for attaining global food security. This requires breeding resilient wheat cultivars that are resistant/tolerant to major biotic (rust diseases) and abiotic ( $O_3$ ) stresses, while maintaining high yield. This research characterized the  $O_3$  responses of wheat genotypes that serve critical roles in developing new rust resistant cultivars. This information will contribute to the simultaneous breeding for rust resistance and  $O_3$  tolerance.

**Author Contributions:** Conceptualization, A.M.M., K.O.B., C.J.S. and D.S.M.; formal analysis and investigation, A.M.M., K.O.B., D.S.M., C.J.S., A.S.A. and R.; resources, D.S.M., K.O.B. and A.M.M.; writing—original draft preparation, A.M.M., C.J.S., K.O.B., and D.S.M.; writing—review and editing, A.M.M., C.J.S., K.O.B., D.S.M., A.S.A. and R. All authors have read and agreed to the published version of the manuscript.

**Funding:** A.M.M. was supported by a PhD scholarship (Governmental Mission No.980) sponsored by the Cultural Affairs and Mission Sector, Ministry of Higher Education and Research, Egypt. This research received no further external funding.

**Acknowledgments:** The authors thank Yue Jin, Samuel Gale, Cereal Disease Laboratory, USDA-ARS, Harold Bockelman, National Small Grains Collection, U.S. Department of Agriculture-Agricultural Research Service and Cristina Cowger, Department of Entomology and Plant pathology, for providing the seeds of the tested genotypes. The authors also thank Samuel Ray, Walter Pursley, Jeff Barton, L. Renee Tucker, Amanda Roth and Megan Reavis for their assistance with  $O_3$  exposure and data collection.

**Conflicts of Interest:** The authors declare no conflict of interest. The funders had no role in the design of the study; in the collection, analyses, or interpretation of data; in the writing of the manuscript, or in the decision to publish the results.

## Appendix A

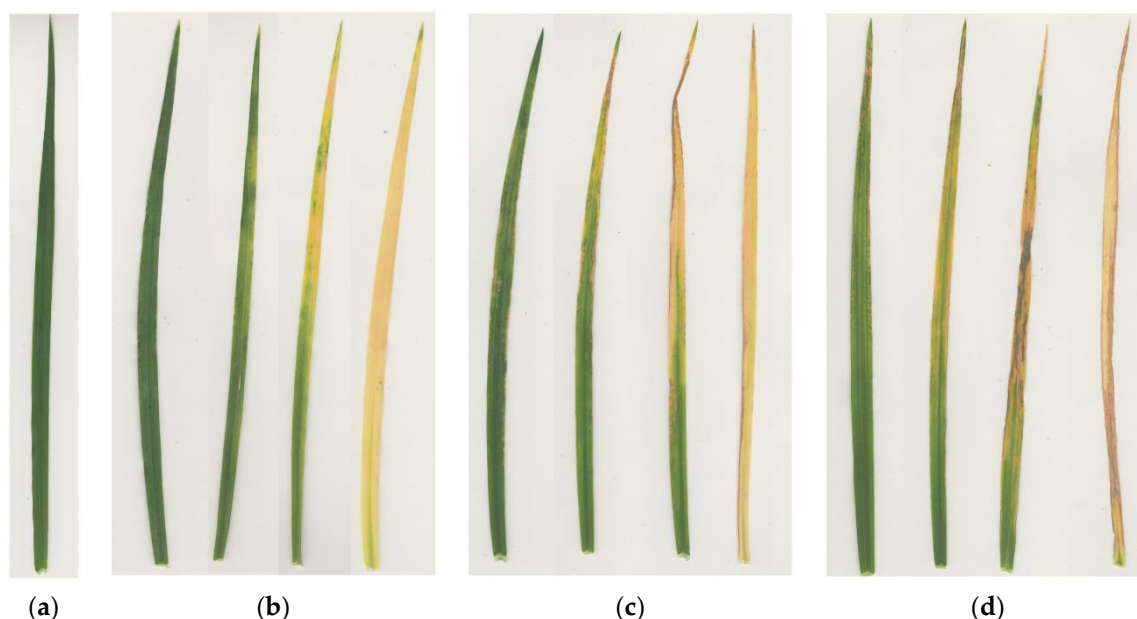


**Figure A1.** Untreated third leaf of Thatcher at charcoal filtered air (a) and third leaves selected from eight rust near-universal susceptible genotypes (Chinese Spring, Line E, Little Club, LMPG 6, McNair 701, Morocco, Rusty, and Thatcher,) showing different levels and types of  $O_3$  injury at three  $O_3$  treatments: 50 ppb (b); 70 ppb (c); 90 ppb (d), exposed for 14 days (12 h/day), at 25 °C and 50% RH, in OPECs.

## References

1. Chakraborty, S.; Luck, J.; Hollaway, G.; Fitzgerald, G.; White, N. Rust-proofing wheat for a changing climate. *Euphytica* **2011**, *179*, 19–32. [CrossRef]
2. Mills, G.; Sharps, K.; Simpson, D.; Pleijel, H.; Broberg, M.; Uddling, J.; Jaramillo, F.; Davies, W.J.; Dentener, F.; Van den Berg, M.; et al. Ozone pollution will compromise efforts to increase global wheat production. *Glob. Chang. Biol.* **2018**, *24*. [CrossRef] [PubMed]
3. Jin, Y.; Rouse, M.; Groth, J. Population Diversity of *Puccinia graminis* is Sustained Through Sexual Cycle on Alternate Hosts. *J. Integr. Agric.* **2014**, *13*, 262–264. [CrossRef]
4. Sharma, J.S.; Zhang, Q.; Rouse, M.N.; Klindworth, D.L.; Friesen, T.L.; Long, Y.; Olivera, P.D.; Jin, Y.; McClean, P.E.; Xu, S.S. Mapping and characterization of two stem rust resistance genes derived from cultivated emmer wheat accession PI 193883. *Theor. Appl. Genet.* **2019**, *132*, 3177–3189. [CrossRef]
5. Zhang, P.; Yin, G.; Zhou, Y.; Qi, A.; Gao, F.; Xia, X.; He, Z.; Li, Z.; Liu, D. QTL Mapping of Adult-Plant Resistance to Leaf Rust in the Wheat Cross Zhou 8425B/Chinese Spring Using High-Density SNP Markers. *Front. Plant Sci.* **2017**, *8*. [CrossRef]
6. McIntosh, R.A.; Wellings, C.R.; Park, R.F. *Wheat Rusts: An Atlas of Resistance Genes*; CSIRO Publishing: Melbourne, Australia, 1995.
7. Sandermann, H.; Ernst, D.; Heller, W.; Langebartels, C. Ozone: An abiotic elicitor of plant defence reactions. *Trends Plant Sci.* **1998**, *3*, 47–50. [CrossRef]
8. Jacob, D.J. Introduction to Atmospheric Chemistry. Available online: <http://app.knovel.com/hotlink/toc/id:kpIAC00011/introduction-atmospheric/introduction-atmospheric> (accessed on 23 November 2020).
9. Iriti, M.; Faoro, F. Oxidative Stress, the Paradigm of Ozone Toxicity in Plants and Animals. *Water Air Soil Pollut.* **2007**, *187*, 285–301. [CrossRef]
10. Fares, S.; Weber, R.; Park, J.-H.; Gentner, D.; Karlik, J.; Goldstein, A.H. Ozone deposition to an orange orchard: Partitioning between stomatal and non-stomatal sinks. *Environ. Pollut.* **2012**, *169*, 258–266. [CrossRef]
11. Pellinen, R.; Palva, T.; Kangasjärvi, J. Subcellular localization of ozone-induced hydrogen peroxide production in birch (*Betula pendula*) leaf cells. *Plant J.* **1999**, *20*, 349–356. [CrossRef]
12. Vahisalu, T.; Puzõrjova, I.; Brosché, M.; Valk, E.; Lepiku, M.; Moldau, H.; Pechter, P.; Wang, Y.; Lindgren, O.; Salojärvi, J.; et al. Ozone-triggered rapid stomatal response involves the production of reactive oxygen species, and is controlled by *SLAC1* and *OST1*. *Plant J. Cell Mol. Biol.* **2010**, *62*, 442. [CrossRef]
13. Altimir, N.; Kolari, P.; Tuovinen, J.P.; Vesala, T.; Bäck, J.; Suni, T.; Kulmala, M.; Hari, P. Foliage surface ozone deposition: A role for surface moisture? *Biogeosciences* **2006**, *3*, 209–228. [CrossRef]
14. Singh, S.; Agrawal, S.B. Impact of tropospheric ozone on wheat (*Triticum aestivum* L.) in the eastern Gangetic plains of India as assessed by ethylenediurea (EDU) application during different developmental stages. *Agric. Ecosyst. Environ.* **2010**, *138*, 214–221. [CrossRef]
15. Biswas, D.K.; Xu, H.; Li, Y.G.; Sun, J.Z.; Wang, X.Z.; Han, X.G.; Jiang, G.M. Genotypic differences in leaf biochemical, physiological and growth responses to ozone in 20 winter wheat cultivars released over the past 60 years. *Glob. Chang. Biol.* **2008**, *14*, 46–59. [CrossRef]
16. Pleijel, H.; Eriksen, A.B.; Danielsson, H.; Bondesson, N.; Selldén, G. Differential ozone sensitivity in an old and a modern Swedish wheat cultivar—Grain yield and quality, leaf chlorophyll and stomatal conductance. *Environ. Exp. Bot.* **2006**, *56*, 63–71. [CrossRef]
17. Feng, Z.; Tang, H.; Uddling, J.; Pleijel, H.; Kobayashi, K.; Zhu, J.; Oue, H.; Guo, W. A stomatal ozone flux–response relationship to assess ozone-induced yield loss of winter wheat in subtropical China. *Environ. Pollut.* **2012**, *164*, 16–23. [CrossRef]
18. Hassan, I.A. Interactive Effects of Salinity and Ozone Pollution on Photosynthesis, Stomatal Conductance, Growth, and Assimilate Partitioning of Wheat (*Triticum aestivum* L.). *Photosynthetica* **2004**, *42*, 111–116. [CrossRef]
19. Tiedemann, A.v.; Pfähler, B. Growth stage-dependent effects of ozone on the permeability for ions and non-electrolytes of wheat leaves in relation to the susceptibility to *Septoria nodorum* Berk. *Physiol. Mol. Plant Pathol.* **1994**, *45*, 153–167. [CrossRef]
20. Meyer, U.; Köllner, B.; Willenbrink, J.; Krause, G.H.M. Effects of different ozone exposure regimes on photosynthesis, assimilates and thousand grain weight in spring wheat. *Agric. Ecosyst. Environ.* **2000**, *78*, 49–55. [CrossRef]

21. Biswas, D.K.; Xu, H.; Li, Y.G.; Ma, B.L.; Jiang, G.M. Modification of photosynthesis and growth responses to elevated CO<sub>2</sub> by ozone in two cultivars of winter wheat with different years of release. *J. Exp. Bot.* **2013**, *64*, 1485–1496. [CrossRef]
22. Wattal, R.K.; Siddiqui, Z.H. Effect of Elevated Levels of Carbon Dioxide on the Activity of RuBisCO and Crop Productivity. In *Crop Production and Global Environmental Issues*; Hakeem, K.R., Ed.; Springer International Publishing: Berlin/Heidelberg, Germany, 2015; pp. 241–256.
23. Burkart, S.; Bender, J.; Tarkotta, B.; Faust, S.; Castagna, A.; Ranieri, A.; Weigel, H.-J. Effects of Ozone on Leaf Senescence, Photochemical Efficiency and Grain Yield in Two Winter Wheat Cultivars. *J. Agron. Crop Sci.* **2013**, *199*, 275–285. [CrossRef]
24. Gelang, J.; Pleijel, H.; Sild, E.; Danielsson, H.; Younis, S.; Selldén, G. Rate and duration of grain filling in relation to flag leaf senescence and grain yield in spring wheat (*Triticum aestivum*) exposed to different concentrations of ozone. *Physiol. Plant.* **2000**, *110*, 366–375. [CrossRef]
25. Ojanpera, K.; Patsikka, E.; Ylaranta, T. Effects of low ozone exposure of spring wheat on net CO<sub>2</sub> uptake, Rubisco, leaf senescence and grain filling. *New Phytol.* **1998**, *138*, 451–460. [CrossRef]
26. Mashaheet, A.M.; Burkey, K.O.; Marshall, D.S. Chromosome location contributing to ozone tolerance in wheat. *Plants* **2019**, *8*, 261. [CrossRef] [PubMed]
27. Amundson, R.G.; Kohut, R.J.; Schoettle, A.W.; Raba, R.M.; Reich, P.B. Correlative Reductions in Whole-Plant Photosynthesis and Yield of Winter Wheat Caused by Ozone. *Phytopathology* **1987**, *77*, 75–79. Available online: [https://www.apsnet.org/publications/phytopathology/backissues/Documents/1987Articles/Phyto77n01\\_75.PDF](https://www.apsnet.org/publications/phytopathology/backissues/Documents/1987Articles/Phyto77n01_75.PDF) (accessed on 23 November 2020). [CrossRef]
28. Heagle, A.S.; Miller, J.E.; Pursley, W.A. Growth and yield responses of winter wheat to mixtures of ozone and carbon dioxide. *Crop Sci.* **2000**, *40*, 1656–1664. [CrossRef]
29. Van Dingenena, R.; Dentenera, F.J.; Raesa, F.; Krol, M.C.; Emberson, L.; Cofala, J. The global impact of ozone on agricultural crop yields under current and future air quality legislation. *Atmos. Environ.* **2009**, *43*, 604–618. [CrossRef]
30. Guarin, J.R.; Kassie, B.; Mashaheet, A.M.; Burkey, K.; Asseng, S. Modeling the effects of tropospheric ozone on wheat growth and yield. *Eur. J. Agron.* **2019**, *105*, 13–23. [CrossRef]
31. Pleijel, H.; Broberg, M.C.; Uddling, J.; Mills, G. Current surface ozone concentrations significantly decrease wheat growth, yield and quality. *Sci. Total Environ.* **2018**, *613–614*, 687–692. [CrossRef]
32. Mills, G.; Sharps, K.; Simpson, D.; Pleijel, H.; Frei, M.; Burkey, K.; Emberson, L.; Uddling, J.; Broberg, M.; Feng, Z.; et al. Closing the global ozone yield gap: Quantification and cobenefits for multistress tolerance. *Glob. Chang. Biol.* **2018**, *24*, 4869–4893. [CrossRef]
33. Schauburger, B.; Rolinski, S.; Schaphoff, S.; Müller, C. Global historical soybean and wheat yield loss estimates from ozone pollution considering water and temperature as modifying effects. *Agric. For. Meteorol.* **2019**, *265*, 1–15. [CrossRef]
34. Biswas, D.K.; Xu, H.; Li, Y.G.; Liu, M.Z.; Chen, Y.H.; Sun, J.Z.; Jiang, G.M. Assessing the genetic relatedness of higher ozone sensitivity of modern wheat to its wild and cultivated progenitors/relatives. *J. Exp. Bot.* **2008**, *59*, 951–963. [CrossRef] [PubMed]
35. Broberg, M.C.; Feng, Z.; Xin, Y.; Pleijel, H. Ozone effects on wheat grain quality—A summary. *Environ. Pollut.* **2015**, *197*, 203–213. [CrossRef] [PubMed]
36. Feng, Z.; Kobayashi, K.; Ainsworth, E.A. Impact of elevated ozone concentration on growth, physiology, and yield of wheat (*Triticum aestivum* L.): A meta-analysis. *Glob. Chang. Biol.* **2008**, *14*, 2696–2708. [CrossRef]
37. Feng, Z.; Kobayashi, K. Assessing the impacts of current and future concentrations of surface ozone on crop yield with meta-analysis. *Atmos. Environ.* **2009**, *43*, 1510–1519. [CrossRef]
38. Barnes, J.; Bender, J.; Lyons, T.; Borland, A. Natural and man-made selection for air pollution resistance. *J. Exp. Bot.* **1999**, *50*, 1423–1435. [CrossRef]
39. Comis, D. Breeding Plants for a High-Ozone World. *Agric. Res.* **2011**, *59*, 14. Available online: <https://agresearchmag.ars.usda.gov/AR/archive/2011/Jul/plants0711.pdf> (accessed on 23 November 2020).
40. Ainsworth, E.A.; Rogers, A.; Leakey, A.D.B. Targets for Crop Biotechnology in a Future High-CO<sub>2</sub> and High-O<sub>3</sub> World. *Plant Physiol.* **2008**, *147*, 13–19. [CrossRef]
41. Rogers, H.H.; Jeffries, H.E.; Stahel, E.P.; Heck, W.W.; Ripperton, L.A.; Witherspoon, A.M. Measuring Air Pollutant Uptake by Plants: A Direct Kinetic Technique. *J. Air Pollut. Control Assoc.* **1977**, *27*, 1192. [CrossRef]

42. Heck, W.W.; Dunning, J.A.; Philbeck, R.B. *A Continuous Stirred Tank Reactor (CSTR) System for Exposing Plants to Gaseous Air Contaminants: Principles, Specifications, Construction, and Operation*; Department of Agriculture, Agricultural Research Service, Southern Region: New Orleans, LA, USA, 1978.
43. Flowers, M.D.; Fiscus, E.L.; Burkey, K.O.; Booker, F.L.; Dubois, J.-J.B. Photosynthesis, chlorophyll fluorescence, and yield of snap bean (*Phaseolus vulgaris* L.) genotypes differing in sensitivity to ozone. *Environ. Exp. Bot.* **2007**, *61*, 190–198. [[CrossRef](#)]
44. Begum, H.; Alam, M.S.; Feng, Y.; Koua, P.; Ashrafuzzaman, M.; Shrestha, A.; Kamruzzaman, M.; Dadshani, S.; Ballvora, A.; Naz, A.A. Genetic dissection of bread wheat diversity and identification of adaptive loci in response to elevated tropospheric ozone. *Plant. Cell Environ.* **2020**, 1–16. [[CrossRef](#)]
45. Quarrie, S.A.; Kaminska, A.; Dodmani, A.; González, I. QTLs governing ozone impacts on wheat yield. *Comp. Biochem. Physiol. Part A Mol. Integr. Physiol.* **2007**, *146*, S261. [[CrossRef](#)]
46. Morgounov, A.; Tufan, H.A.; Sharma, R.; Akin, B.; Bagci, A.; Braun, H.-J.; Kaya, Y.; Keser, M.; Payne, T.S.; Sonder, K.; et al. Global incidence of wheat rusts and powdery mildew during 1969–2010 and durability of resistance of winter wheat variety Bezostaya 1. *Eur. J. Plant Pathol.* **2012**, *132*, 323–340. [[CrossRef](#)]
47. McDonald, B.A.; Linde, C. Pathogen population genetics, evolutionary potential, and durable resistance. *Annu. Rev. Phytopathol.* **2002**, *40*, 349–379. [[CrossRef](#)] [[PubMed](#)]
48. Kolmer, J.A. Tracking wheat rust on a continental scale. *Curr. Opin. Plant Biol.* **2005**, *8*, 441–449. [[CrossRef](#)] [[PubMed](#)]
49. Ali, I. Inheritance of Leaf Rust Resistance in Wheat Cultivars Morocco and Little Club. *Plant Dis.* **1994**, *78*, 383. [[CrossRef](#)]
50. Zeven, A.C. Fifth supplementary list of wheat varieties classified according to their genotype for hybrid necrosis and geographical distribution of Ne-genes. *Euphytica* **1971**, *20*, 239–254. [[CrossRef](#)]
51. Luig, N.H. *A Survey of Virulence Genes in Wheat Stem Rust, Puccinia Graminis f. sp. Tritici*; Advances i. Berlin, Hamburg; Verlag Paul Parey: Berlin, Germany, 1983.
52. Knott, D.R. Agronomic and quality characters of near-isogenic lines of wheat carrying genes for stem rust resistance. *Euphytica* **1993**, *68*, 33–41. [[CrossRef](#)]
53. Middleton, G.K.; Bennett, J.R.; Newton, H.C. Registration of McNair 701 Wheat. *Crop Sci.* **1973**, *13*, 585. [[CrossRef](#)]
54. Zadoks, J.C.; Chang, T.T.; Konzak, C.F. A decimal code for the growth stages of cereals. *Weed Res.* **1974**, *14*, 415–421. [[CrossRef](#)]
55. Mashaheet, A.M.S. Effects of Near-Ambient O<sub>3</sub> and CO<sub>2</sub> on Wheat Performance and Interactions with Leaf and Stem Rust Pathogens. Ph.D. Thesis, North Carolina State University, Raleigh, NC, USA, 2016.
56. Bergmann, E.; Bender, J.; Weigel, H.J. Impact of tropospheric ozone on terrestrial biodiversity: A literature analysis to identify ozone sensitive taxa. *J. Appl. Bot. Food Qual.* **2017**, *90*, 11–21. [[CrossRef](#)]
57. Mills, G.; Hayes, F.; Simpson, D.; Emberson, L.; Norris, D.; Harmens, H.; Büker, P. Evidence of widespread effects of ozone on crops and (semi-)natural vegetation in Europe (1990–2006) in relation to AOT40- and flux-based risk maps. *Glob. Chang. Biol.* **2011**, *17*, 592–613. [[CrossRef](#)]
58. Dohmen, G.P. Secondary effects of air pollution: Ozone decreases brown rust disease potential in wheat. *Environ. Pollut.* **1987**, *43*, 189–194. [[CrossRef](#)]
59. Heagle, A.S.; Key, L.W. Effect of *Puccinia graminis* f. sp. *tritici* on Ozone Injury in Wheat. *Phytopathology* **1973**, *63*, 609. [[CrossRef](#)]
60. Helfer, S. Rust fungi and global change. *New Phytol.* **2014**, *201*, 770–780. [[CrossRef](#)]
61. Tiedemann, A.; Weigel, H.J.-J.; Jäger, H.J.-J. Effects of open-top chamber fumigations with ozone on three fungal leaf diseases of wheat and the mycoflora of the phyllosphere. *Environ. Pollut.* **1991**, *72*, 205–224. [[CrossRef](#)]
62. Tiedemann, A. Ozone Effects on Fungal Leaf Diseases of Wheat in Relation to Epidemiology. II. Biotrophic Pathogens. *J. Phytopathol. Z.* **1992**, *134*, 187–197.
63. Tiedemann, A.V.; Firsching, K.H.; Tiedemann, A.V.; Firsching, K.H. Interactive effects of elevated ozone and carbon dioxide on growth and yield of leaf rust-infected versus non-infected wheat. *Environ. Pollut.* **2000**, *108*, 357–363. [[CrossRef](#)]
64. Mayer, K.F.X.; Rogers, J.; Doležel, J.; Pozniak, C.J.; IWGSC. A chromosome-based draft sequence of the hexaploid bread wheat (*Triticum aestivum*) genome. *Science* **2014**, *345*, 1251788. [[CrossRef](#)]

65. Quarrie, S.A.; Steed, A.; Calestani, C.; Semikhodskii, A.; Lebreton, C.; Chinoy, C.; Steele, N.; Pljevljakusić, D.; Waterman, E.; Weyen, J.; et al. A high-density genetic map of hexaploid wheat (*Triticum aestivum* L.) from the cross Chinese Spring × SQ1 and its use to compare QTLs for grain yield across a range of environments. *Theor. Appl. Genet.* **2005**, *110*, 865–880. [[CrossRef](#)]
66. Quarrie, S.A.; Gulli, M.; Calestani, C.; Steed, A.; Marmiroli, N. Location of a gene regulating drought-induced abscisic acid production on the long arm of chromosome 5A of wheat. *Theor. Appl. Genet.* **1994**, *89*, 794–800. [[CrossRef](#)]
67. Hiebert, C.W.; Kolmer, J.A.; McCartney, C.A.; Briggs, J.; Fetch, T.; Bariana, H. Major Gene for Field Stem Rust Resistance Co-Locates with Resistance Gene *Sr12* in ‘Thatcher’ Wheat. *PLoS ONE* **2016**, *11*, e0157029. [[CrossRef](#)] [[PubMed](#)]

**Publisher’s Note:** MDPI stays neutral with regard to jurisdictional claims in published maps and institutional affiliations.



© 2020 by the authors. Licensee MDPI, Basel, Switzerland. This article is an open access article distributed under the terms and conditions of the Creative Commons Attribution (CC BY) license (<http://creativecommons.org/licenses/by/4.0/>).